Resting Myoplasmic Free Calcium in Frog Skeletal Muscle Fibers Estimated with Fluo-3

A. B. Harkins, Nagomi Kurebayashi,‡ and S. M. Baylor
Department of Physiology, University of Pennsylvania School of Medicine, Philadelphia, Pennsylvania 19104-6085 USA

ABSTRACT Fluo-3 is an unusual tetracarboxylate Ca^{2+} indicator. For recent lots supplied by Molecular Probes Inc. (Eugene, OR), F_{MAX}, the fluorescence intensity of the indicator in its Ca^{2+}-bound form, is ~200 times that of F_{MIN}, the fluorescence intensity of the indicator in its Ca^{2+}-free form. (For earlier lots, impurities may account for the smaller reported values of F_{MAX}/F_{MIN}, 36–40). We have injected fluo-3 from a high-purity lot into intact single fibers from frog muscle and measured the indicator's absorbance and fluorescence signals at rest (A and F, respectively) and changes in absorbance and fluorescence following action potential stimulation (ΔA and ΔF, respectively). As for other high-affinity Ca^{2+} indicators used previously in frog muscle, the time course of the indicator's ΔA and ΔF signals substantially lagged behind that of the myoplasmic free Ca^{2+} transient. Our analysis of fluo-3's signals from myoplasm therefore focused on information about the level of resting myoplasmic free $[Ca^{2+}]$ ($[Ca^{2+}]_r$).

From A, ΔA, and in vitro estimates of fluo-3's molar extinction coefficients, the change in the fraction of fluo-3 in the Ca^{2+}-bound form during activity (Δf) was estimated. From Δf, ΔF, and F, the fraction of the indicator in the Ca^{2+}-bound form in the resting fiber (f_r) was estimated by $f_r = (\Delta f \times F/\Delta F) + (1 - F_{MAX}/F_{MIN})^{-1}$. Since F_{MAX}/F_{MIN} is large, the contribution of the second term to the estimate of f_r is small. At 16°C, the mean value (mean ± S.E.) of f_r was 0.086 ± 0.004 (N = 15). From two estimates of the apparent dissociation constant of fluo-3 for Ca^{2+} in the myoplasm, 1.09 and 2.57 μM, the average value of $[Ca^{2+}]_r$ is calculated to be 0.10 and 0.24 μM, respectively. The smaller of these estimates lies near the upper end of the range of values for $[Ca^{2+}]_r$ in frog fibers (0.02–0.12 μM) estimated by others with aequorin and Ca^{2+}-selective electrodes. The larger of the estimates lies within the range of values (0.2–0.3 μM) previously estimated in this laboratory with fura red. We conclude that $[Ca^{2+}]_r$ in frog fibers is at least 0.1 μM and possibly as large as 0.3 μM.

INTRODUCTION

A recent article from this laboratory (1) described the use of the Ca^{2+} indicator fura red (2) to estimate the resting level of myoplasmic free $[Ca^{2+}]$ ($[Ca^{2+}]_r$) in intact frog skeletal muscle fibers. The value estimated, 0.2–0.3 μM, is higher than the 0.02–0.12 μM range previously estimated with aequorin and Ca^{2+}-selective microelectrodes (Ref. 3 and other references cited in Ref. 1). Our goal here was to see if fluo-3 (4), an indicator that produces a very large increase in fluorescence intensity upon complexation with Ca^{2+}, might also be used to estimate $[Ca^{2+}]_r$. Since neither the excitation nor emission spectrum of fluo-3 changes substantially with Ca^{2+} complexation, it is not possible to calibrate this indicator's signal by commonly employed "ratiometric" procedures, e.g., those used with indo-1 and fura-2 (5). Moreover, since the fractional change in fluo-3's absorbance spectrum with Ca^{2+} complexation is small, calibration by the procedure developed for fura red in frog fibers (1), which utilizes information in the shape of the indicator's resting absorbance spectrum, is also not possible.

We report here a novel calibration procedure for estimation of $[Ca^{2+}]_r$ with fluo-3. The method relies on the measurement of the indicator's absorbance and fluorescence signals in a fiber at rest (signals denoted A and F, respectively) and changes in these signals following electrical stimulation (ΔA and ΔF). From these four in vivo measurements, from in vitro estimates of the indicator's molar extinction coefficients in its Ca^{2+}-free and Ca^{2+}-bound forms, and from an assumed value for F_{MAX}/F_{MIN} (the ratio of the fluorescence intensity of Ca^{2+}-bound fluo-3 to that of Ca^{2+}-free fluo-3), it is possible to estimate f_r, the fraction of fluo-3 in the Ca^{2+}-bound form at rest. Because the value of F_{MAX}/F_{MIN} in myoplasm is likely to be large (≥100), the estimate of f_r is not very sensitive to the exact value assumed for F_{MAX}/F_{MIN}.

In these experiments, which utilized a nonperturbing concentration of indicator (≤ 0.2 mM), the average value estimated for f_r was 0.086 (± 0.004, mean ± S.E.; N = 15; 16°C). From two estimates of fluo-3's dissociation constant for Ca^{2+} in the myoplasmic environment, 1.09 and 2.57 μM, the corresponding estimates of $[Ca^{2+}]_r$ are 0.10 and 0.24 μM. The smaller of these estimates falls near the upper end of the range of $[Ca^{2+}]_r$ (0.02–0.12 μM) previously obtained with the other techniques, while the larger of the estimates agrees with our estimates obtained with fura red, 0.2–0.3 μM (1). The results support the conclusion that $[Ca^{2+}]_r$ is likely to be at least 0.1 μM and possibly as large as 0.3 μM.

Some of the results have been presented previously in abstract form (6–8).

METHODS

The penta-ammonium salt of fluo-3 was obtained from Molecular Probes, Inc. (Eugene, OR) and stored in a freezer until use, when a stock solution

Received for publication 1 February 1993 and in final form 16 April 1993.

Address reprint requests to Dr. S. M. Baylor, Department of Physiology, University of Pennsylvania School of Medicine, Philadelphia, PA 19104–6085.

‡Current address: Department of Pharmacology, Juntendo University School of Medicine, 2-1-1 Hongo, Bunkyo-ku, Tokyo 113, Japan.

0006-3495/93/08/865/17 $2.00

of 10–30 mM fluo-3 in distilled water was prepared. For the in vitro measurements, this solution was diluted into the various buffer solutions to a final concentration of 0.01–0.1 mM. For the in vivo measurements, the stock solution itself was pressure-injected into single muscle fibers. With lot 10B-1 (an early lot of fluo-3 from Molecular Probes), the value of F_{MAX}/F_{MIN} measured in vitro was ~40, as expected from the report of Minta et al. (4). With a more recent lot (lot 10D-1), however, F_{MAX}/F_{MIN} was much larger, ~200 (see Results). Chemical analysis indicated that the purity of lot 10D-1 was high: ~95% of the total absorbance of a sample (measured at 500 nm) eluted as a single peak when analyzed by liquid chromatography (Waters HPLC System; Milford, MA). Unless indicated otherwise, all measurements reported in Results were carried out with lot 10D-1. The methods used were similar to those previously described (1, 9) and are summarized below. All measurements, both in vitro and in vivo, were carried out at 16–17°C.

In vitro measurements

Solutions

Buffer alone. A standard buffer solution was used to characterize the basic absorbance and fluorescence properties of fluo-3. This solution contained (in millimolar): 97.7 KCl, 10 PIPES (piperazine-*N*,*N*'-bis(2-ethanesulfonic acid)) and either 10 EGTA (ethyleneglycol-bis(β-aminoethyl ether)-*N*,*N*,*N*',*N*'-tetraacetic acid), which was used for the Ca^{2+}-free calibration solution ("0 Ca^{2+}" solution), or 10 $CaCl_2$, which was used for the saturating-Ca^{2+} calibration solution ("sat. Ca^{2+}" solution). The ionic strength was 0.15 M and, unless indicated otherwise, the pH was 7.03.

Buffer plus sucrose. To characterize effects of solution viscosity (reported in centipoise, cP), measurements were made in the standard buffer with either no added sucrose (viscosity = 1.1 cP) or with 0.632 M sucrose (viscosity = 2.2 cP, referred to hereafter as the 2 cP buffer solution). The viscosity of these solutions at 16°C was estimated from standard tables.

Buffer plus aldolase. To characterize possible effects of myoplasmic proteins, measurements were made in buffer solution containing aldolase, the most abundant soluble myoplasmic protein on a weight basis (10). Rabbit aldolase (type "X," molecular weight 160,000, lots 40H9570 and 120H9500; Sigma Chemical Co., St. Louis, MO) was prepared as described previously (1, 9) and used at concentrations between 0 and 122 mg/ml. In some experiments, solution viscosity was maintained approximately constant (at 2 cP) as the aldolase concentration was increased, by proportional reductions in the sucrose concentration. The viscosity of these solutions was estimated from previous calibrations (9), carried out with an Ostwald-type viscometer, on solutions of similar composition.

Optical measurements

Absorbance. In vitro absorbance spectra of 10–20 μM Fluo-3 were measured in a spectrophotometer (Ultraspec 4050; LKB Instruments, Gaithersburg, MD) at wavelengths λ between 400 and 600 nm (in 2-nm increments). The spectra were later interpolated to 1-nm resolution and filtered by an 11-point smoothing routine that averaged absorbance over 11 adjacent wavelengths. The filtered curves could then be compared with the fiber absorbance measurements (see below), which were made with interference filters that had a 10-nm bandpass (Omega Optical Co., Brattleborough, VT). In the standard buffer solution (1.1 cP), the isosbestic wavelengths for Fluo-3's reaction with Ca^{2+} were found to be 503 and 530 nm. The molar extinction coefficient at 503 nm (ϵ_{503}) was estimated to be 8.19×10^4 M^{-1} cm^{-1} from the following information: (*a*) the value of ϵ_{506}, 8.35×10^4 M^{-1} cm^{-1}, given by Minta et al. (4) for the Ca^{2+}-bound form of Fluo-3 in a solution of similar viscosity and (*b*) the ratio of absorbances at 503 and 506 nm measured from Fluo-3's sat. Ca^{2+} spectrum. This value of ϵ_{503} was then used as a standard for calculation of molar extinction coefficients at other wavelengths and under other solution conditions (see below).

Fluorescence. Quartz capillaries (internal diameter, 150–230 μm; Vitro Dynamics, Rockaway, NJ) were filled with buffer solution containing 0.06–0.10 mM Fluo-3 and mounted on the horizontal optical bench apparatus used for the muscle fiber experiments (11). Fluorescence was excited with light of wavelength 480 ± 15 nm, selected by an interference filter (RDF480 filter; Omega Optical Co.) positioned between the 100-W tungsten-halogen source and the capillary. Emission wavelengths greater than 510 nm were selected by a barrier filter (REF510; Omega Optical Co.) placed between the capillary and the silicon diode (UV100; EG&G, Salem, MA) used to measure light intensity. In all cases the reported Fluorescence intensities (F) have been corrected for a small component of nonFluorescent light ("cross-talk" intensity) that arose because of an overlap in the bandpass of the excitation and emission filters.

Inner filter effect calculations. Calculations of the type described in Ref. 1 were made to check whether, as a result of the inner filter effect (12), the ratio F_{MAX}/F_{MIN} is expected to vary significantly with the concentration of Fluo-3. The calculations indicated that variations in F_{MAX}/F_{MIN} should be small (≤ 1%) at the principal indicator concentrations used in this paper (in vitro, ≤ 0.1 mM; in vivo, ≤ 0.2 mM). Experimental checks, at Fluo-3 concentrations between 0.01 and 0.3 mM, confirmed that this was the case. Therefore corrections of the type made for fura red (1) were not made for Fluo-3.

Fluorescence emission anisotropy. The anisotropy (denoted *a*) of Fluo-3's Fluorescence emission was measured in the manner described for fura-2 (9) and fura red (1). As expected, *a* for Fluo-3 was found to be essentially the same whether the excitation beam was linearly polarized parallel or perpendicular to the long axis of the capillary (anisotropy values denoted a_0 and a_{90}, respectively); hence, the values of *a* reported in Results are the average of a_0 and a_{90}. To estimate the "limiting anisotropy" of Fluo-3 in a solution of "infinite" viscosity, measurements of *a* were made at solution viscosities between 1.1 and 30 cP (sucrose concentrations between 0 and 1.975 M; cf. Ref. 9) and analyzed by means of a Perrin plot (cf. Refs. 9 and 12).

Estimation of K_D. Fluo-3's apparent dissociation constant for Ca^{2+} (K_D) was estimated from measurements of the Fluorescence intensity of capillary solutions that contained the same concentration of Fluo-3 (0.10 mM) but different concentrations of free Ca^{2+} ($[Ca^{2+}]$). The latter values (reported in pCa units) were set by a Ca^{2+}-EGTA buffer system (1). The intensity data were fitted by the equation for 1:1 binding:

$$f = \frac{[Ca^{2+}]}{[Ca^{2+}] + K_D} \quad (1)$$

with K_D taken as an adjustable parameter. For each $[Ca^{2+}]$ level, *f*, the fraction of Fluo-3 in the Ca^{2+}-bound form, was calculated from the measured value of F by the equation $f = (F - F_{MIN})/(F_{MAX} - F_{MIN})$ (cf. Fig. 4 *A*).

In vivo measurements

Adult frogs (*Rana temporaria*; Charles Sullivan, Nashville, TN) of both sexes were obtained during all seasons of the year and kept in a refrigerator at 4°C. The time spent in the cold before use was typically 2–4 weeks (range, 1–8 weeks). Single twitch fibers from iliofibularis or semitendinosus muscle were dissected in a normal Ringer solution (120 mM NaCl, 2.5 mM KCl, 1.8 mM $CaCl_2$, 5 mM PIPES; pH 7.1). An isolated fiber was mounted on the optical bench apparatus, stretched to a long sarcomere length (3.6–4.0 μm) and lowered onto pedestal supports to minimize movement artifacts in the optical records. Fluo-3 was pressure-injected into the myoplasm after impalement of the fiber by a glass micropipette (tip resistance, ~5 MΩ, if filled with 3 M KCl). In many experiments the injection of indicator proceeded slowly at the pressure most-commonly used (~10 p.s.i.) and, in these experiments, injections took up to 15 min to complete. The volume of fluid injected was typically quite small, less than 10 pL, as calculated from the concentration of indicator in the pipette and the profile of indicator concentration measured along the fiber axis. Swelling of the fiber at the injection site was generally not observed.

In some experiments, the normal Ringer solution was exchanged for a "high-Ca^{2+}" Ringer that contained 11.8 rather than 1.8 mM $CaCl_2$. The high Ca^{2+} Ringer appeared to reduce the likelihood of impalement damage that sometimes resulted from the microinjection of indicator (cf. Ref. 13). In three experiments, the normal Ringer solution was exchanged for Ringer containing an elevated concentration of potassium, 5–12.5 mM. In these

experiments, the NaCl was partially replaced with Na^+-proprionate so that the KCl product, and the ionic strength of the Ringer remained approximately constant (cf. Ref. 3).

Criteria for a successful injection. To assess possible fiber damage related to the injection of indicator, the fiber's intrinsic birefringence signal in response to action potential stimulation ("second component" described in Ref. 14) was measured before and after the injection. A fiber was not included in the analysis unless its birefringence signal was of normal appearance (fractional change in light intensity, ≥ 0.001; time to peak, 8–10 ms) and essentially unchanged as a result of the injection. A second assessment of injection damage, carried out immediately after completion of the injection, came from a visual inspection of Fluo-3's resting Fluorescence. In many fibers, a small region of slightly elevated Fluorescence was detected within a 10–20 μm radius of the impalement site; a fiber of this type usually had a normal birefringence signal and, if so, was included in the anaylsis. A few fibers, however, had a larger, more intense and, in some cases, irregular Fluorescence at the impalement site; fibers of this type were assumed to have suffered significant damage as a result of the injection and were excluded from the analysis. In general, the principal optical measurements were made at a location slightly removed from the injection site (e.g., 50–150 μm along the fiber axis) to minimize the possible influence of injection damage on the estimates of $[Ca^{2+}]_r$.

Absorbance measurements. Following a successful injection, a small region of the fiber was transilluminated with a spot of light (diameter, 43–73 μm) for the measurement of fiber absorbance. The measurements and analysis were carried out at a series of wavelengths (480–630 nm, λ increments of 10–30 nm), selected by interference filter (1). The raw measurements were corrected for the estimated contribution of the fiber's intrinsic absorbance to obtain the indicator-related absorbance (denoted $A(\lambda)$; cf. Fig. 5). From $A(\lambda)$, Beer's law was used to estimate the myoplasmic concentration of indicator (denoted $[D_T]$). For this purpose the $A(\lambda)$ data were fitted with the indicator's absorbance spectrum measured in a 0 Ca^{2+} solution. As described in Results, good fits of $A(\lambda)$ were not obtained unless the in vitro spectrum was shifted along the wavelength axis. For the estimation of $[D_T]$, the following molar extinction coefficients (ϵ) and corresponding isosbestic wavelengths (λ_{iso}; referenced to the unshifted wavelength axis) were obtained from the in vitro spectra: (i) for the 2 cP solution with no added protein ("0 aldolase" condition): λ_{iso} = 504 nm and ϵ_{504} = 7.83×10^4 M^{-1} cm^{-1}; (ii) for the "saturating" aldolase condition (see Results): λ_{iso} = 515 nm and $\epsilon_{515} = 6.99 \times 10^4$ M^{-1} cm^{-1}. The myoplasmic path length was estimated as previously described (15).

The change in fiber absorbance in response to action potential stimulation ($\Delta A(\lambda)$) was also measured (1). Interestingly, the $\Delta A(\lambda)$ measurements contained clearly resolved information about the change in concentration of Ca^{2+}-Fluo-3 complex. Thus, the $\Delta A(\lambda)$ measurements provided the additional piece of information required to calibrate the indictor's in vivo signals in terms of absolute $[Ca^{2+}]$ levels (see following paragraphs). Information sufficient for calibration was not available from the resting $A(\lambda)$ measurements because, in our apparatus, two sources of noise rendered unresolvable any potential information about the resting concentration of Ca^{2+}-Fluo-3 complex: (i) the noise introduced by the correction for the fiber's intrinsic absorbance (cf. Fig. 5) and (ii) the noise resulting from fluctuations in lamp intensity that occur on a time scale of several minutes (the time scale required to record the reference intensity levels needed for calculation of $A(\lambda)$).

As for $A(\lambda)$, $\Delta A(\lambda)$ was not well-fitted by an in vitro Ca^{2+}-difference spectrum unless the difference spectrum was shifted along the wavelength axis. From $\Delta A(\lambda)$, Beer's law was used to estimate Δ[CaD], the change in concentration of Ca^{2+}-Fluo-3 complex. For this calculation, changes in the indicator's molar extinction coefficient ($\Delta\epsilon$) were estimated at two wavelengths near the positive and negative peaks of the difference spectrum; the estimation of Δ[CaD] relied on the difference in the two $\Delta\epsilon$ values, as follows: (i) for the 0 aldolase (2 cP) condition: $\Delta\epsilon_{515} - \Delta\epsilon_{493} = 2.50 \times 10^4$ M^{-1} cm^{-1}; (ii) for the saturating aldolase condition: $\Delta\epsilon_{527} - \Delta\epsilon_{501} = 1.86 \times 10^4$ M^{-1} cm^{-1}. From the measurements of $A(\lambda)$ and $\Delta A(\lambda)$, the change in the fraction of Fluo-3 in the Ca^{2+}-bound form (Δf) was estimated as: $\Delta f = \Delta[CaD]/[D_T]$.

Fluorescence measurements. The Fluorescence intensity (F) of Fluo-3 in a resting fiber was measured with the same filters used for the capillary measurements. A vertical slit was usually inserted into the light path to restrict the excitation beam to an axial length of fiber of ~70 μm. As for the in vitro measurements, the F measurements were corrected for the cross-talk component of intensity. This component was estimated from a region of fiber, distant from the injection site, that did not contain indicator. The change in Fluo-3 Fluorescence in response to action potential stimulation (ΔF) was also measured. Since resting F was always measured just prior to stimulation, the fractional change in Fluorescence ($\Delta F/F$) could be calculated.

Estimation of f_r. If Fluo-3 exists in myoplasm in one of two states, Ca^{2+}-free or Ca^{2+}-bound, then F is related to f_r, the fraction of the indicator in the Ca^{2+}-bound form at rest, by:

$$F = F_{MIN} + f_r(F_{MAX} - F_{MIN}) \quad (2)$$

Here, F_{MIN} and F_{MAX} denote the intensity levels that would be measured if all the indicator molecules in the measurement region were either Ca^{2+}-free or Ca^{2+}-bound, respectively. Similarly, ΔF is related to Δf by:

$$\Delta F = \Delta f(F_{MAX} - F_{MIN}). \quad (3)$$

Hence:

$$f_r = \Delta f(F/\Delta F) + (1 - F_{MAX}/F_{MIN})^{-1}. \quad (4)$$

Since $\Delta f = \Delta[CaD]/[D_T]$ (see above), f_r can be calculated from the measurements of A, ΔA, F, ΔF, and an assumed value for F_{MAX}/F_{MIN}. If F_{MAX}/F_{MIN} is large (e.g., in the range 100–200, see Results), the value estimated for f_r is not very sensitive to the exact value assumed for F_{MAX}/F_{MIN}.

For Equation 4 to be accurate, the absorbance and Fluorescence measurements must be made from the same fiber region and referred to the same point in time. The optical measurements were therefore made as follows: (i) $\Delta F/F$ was measured first. (ii) Then $A(\lambda)$ and $\Delta A(\lambda)$ were measured sequentially at five to eight wavelengths between 480 and 630 nm; these measurements were made within the same 70-μm length of fiber used for the Fluorescence measurements and included appropriate bracketing at one or two wavelengths, usually 510 and/or 520 nm. (iii) $\Delta F/F$ was again measured. In the analysis stage, the $A(\lambda)$ and $\Delta A(\lambda)$ data were corrected by interpolation for any small changes in indicator concentration during the run, and the corrected data were compared with the average of the two measurements of $\Delta F/F$. The $\Delta F/F$ amplitudes usually differed by 5–10% (range 0–20%). With each absorbance or Fluorescence measurement in the run, the fiber region received 2–3 s of illumination; the interval between stimulated action potentials was ~30 s.

Statistics. Results from more than two experiments are reported as mean value ± standard error (mean ± SE). Student's two-tailed t test, with $p < 0.05$, was used to determine the statistical significance of a difference between means.

RESULTS

Part I: In vitro measurements

Effects of illumination

To determine whether Fluo-3 was altered by the light intensities available on our apparatus (cf. Ref. 4), capillaries containing the indicator were illuminated continuously with 480 (± 15)-nm light for a period of 10 min, and the values of F measured after 5 and 10 min of illumination were compared with the preillumination level. With the first 5 min of illumination, F_{MIN} and F_{MAX} decreased by 11 and 18%, respectively, and, with the second 5 min of illumination, by a further 0 and 6%, respectively. For the 10-min period, the ratio of F_{MAX}/F_{MIN} decreased, on average, at a rate of ~1.5%/min compared with the preillumination value.

Since, in the in vivo measurements, runs were usually completed with less than 30 s of total illumination (e.g., 5–10 measurements, with 2–3 s of illumination per measurement), alterations in Fluorescence due to illumination during the run are not likely to have been significant.

Effects of viscosity

Although the viscosity of myoplasm is not known precisely, it is probably about twice that of water (2 vs. 1 cP at 20°C (16)). Since a doubling of viscosity was shown to affect somewhat the properties of fura-2 (5, 9, 17) and fura red (1), it was of interest to investigate possible effects of viscosity on Fluo-3.

Absorbance. Absorbance spectra of Fluo-3 were very similar when measured at solution viscosities of 1.1 cP (not shown) and 2 cP (cf. Fig. 1). At the higher viscosity, there appeared to be a small (1–2 nm) red shift in both the 0 Ca^{2+} and sat. Ca^{2+} spectra, with little change (<5%) in spectral amplitude.

Fluorescence. An increase in solution viscosity from 1.1 to 2 cP produced a 19% increase in F_{MIN}, a 3% increase in F_{MAX}, and a 13% decrease in F_{MAX}/F_{MIN}, from 185 to 161.

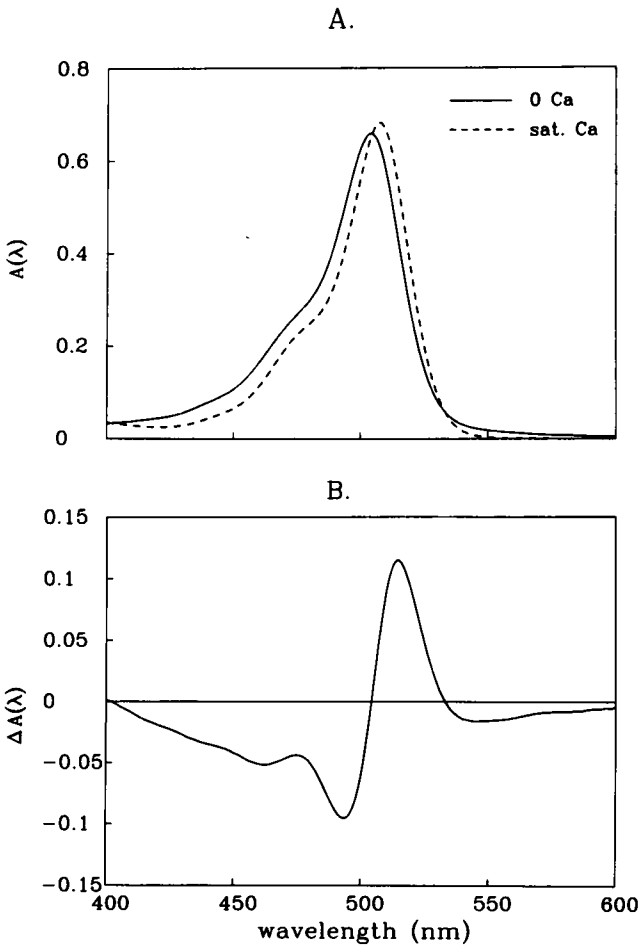

FIGURE 1 In vitro absorbance spectra of 20 μM Fluo-3 measured in a spectrophotometer (solution viscosity of 2 cP, set with sucrose). (*A*) Absolute spectra in 0, and sat. Ca^{2+} solutions. (*B*) The Ca^{2+} difference spectrum (sat. Ca^{2+} minus 0 Ca^{2+}) from *A*, plotted on expanded vertical scale.

Effects of Ca^{2+}

Absorbance. Fig. 1 *A* shows absorbance spectra of Fluo-3 in its Ca^{2+}-free and Ca^{2+}-bound forms. With Ca^{2+} complexation, there is a red-shift of ~3 nm in the location of the peak absorbance and a slight increase in the amplitude of the peak. Fig. 1 *B* shows the Ca^{2+} difference spectrum on expanded vertical scale. This spectrum has an unusual "triphasic" shape, with isosbestic wavelengths at 504 and 535 nm (in a 2-cP solution). Although the fractional change of Fluo-3's absorbance with Ca^{2+} complexation is small, the change is sufficiently large that duplicate measurements of the difference spectrum yielded the same basic shape (cf. the continuous trace in Fig. 2 *E*, described below).

Fluorescence. Minta et al. (4) report that the Fluorescence intensity of Fluo-3 increases ~40-fold with Ca^{2+} complexation (F_{MAX}/F_{MIN} = 36–40). We observed a similar increase for an early sample of Fluo-3 purchased from Molecular Probes (lot 10B-1), in which F_{MAX}/F_{MIN} was ~45 (part A of Table 1). However, for lot 10D-1 (part B of Table 1), F_{MAX}/F_{MIN} was much larger, ~200. When samples from the two lots were examined in parallel measurements at nominally identical concentrations, F_{MAX} of lot 10D-1 was about 1.4 times that of lot 10B-1, whereas F_{MIN} of lot 10D-1 was only one-third that of lot 10B-1. Thus, the nearly 5-fold change in the value of F_{MAX}/F_{MIN} may have been due to a fluorescent contaminant (perhaps a Ca^{2+}-insensitive one) that was present at larger concentration in lot 10B-1. Because a larger value of F_{MAX}/F_{MIN} reduces the uncertainty in the estimate of f_r (cf. Equation 4), lot 10D-1 was routinely used for the measurements of this paper.

Effects of pH

Minta et al. (4) report that, if pH is lowered from 8 to 6, F_{MAX} remains approximately constant, while F_{MIN} increases by a factor slightly less than 2. Table 1 lists values of F_{MAX} and F_{MIN} at three levels of pH (6.8, 7.0, and 7.5) for the two lots of Fluo-3. The variations in F_{MAX} and F_{MIN} with pH are about as expected from the earlier report (4). For a pH change from 7.5 to 6.8, the increase in F_{MIN} was somewhat greater for lot 10D-1 than for lot 10B-1 (relative changes of 46 and 22%, respectively). With lot 10D-1, the average value of F_{MAX}/F_{MIN} measured at all pH values was large, 188–283.

Effects of aldolase

In the case of fura-2 (9, 18) and fura red (1), indicator properties were altered substantially if soluble muscle proteins were added to the calibration solutions at a concentration similar to that of the soluble protein concentration in myoplasm, 50–90 mg/ml (10). It was therefore of interest to determine whether similar effects occurred with Fluo-3. As before, aldolase, the most abundant soluble protein in myoplasm on a weight basis (10), was chosen as a representative protein for these measurements.

Absorbance. Panel *A* of Fig. 2 shows absorbance spectra of Fluo-3 in a 0 Ca^{2+} solution in the absence and presence of 55 mg/ml aldolase. Aldolase caused a red-shift of ~5 nm

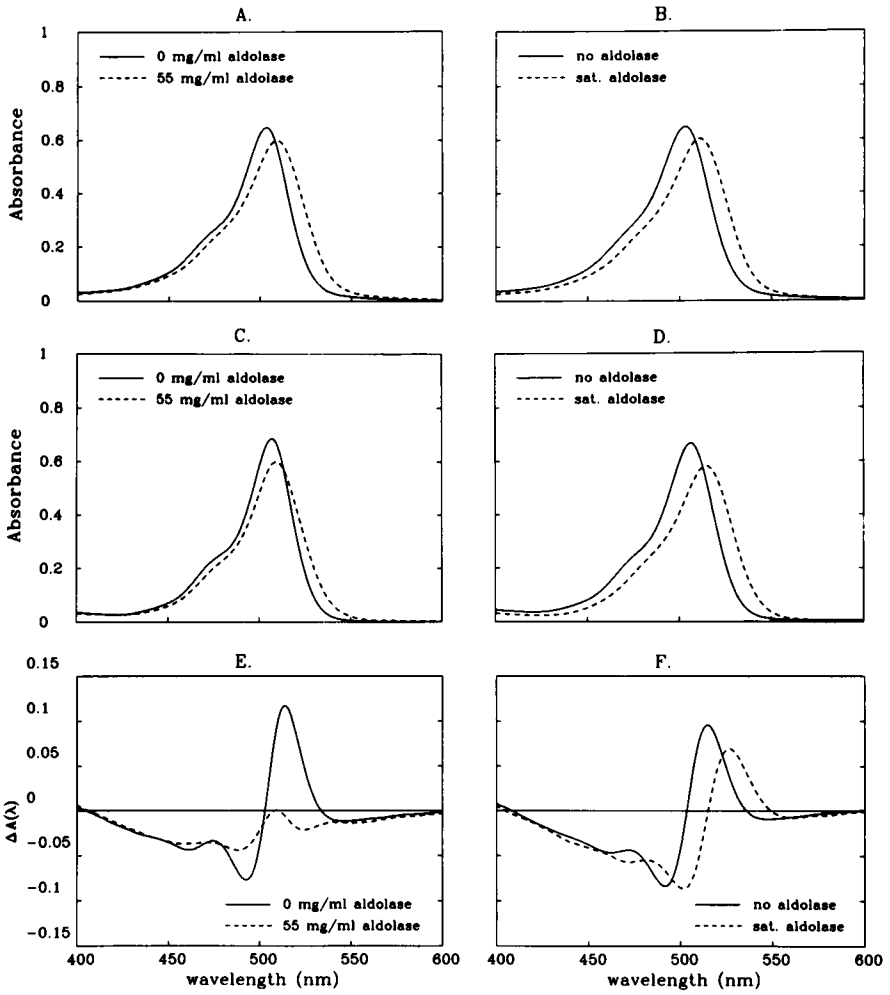

FIGURE 2 Left-hand side (viscosity = 1.6 cP): absorbance spectra of 20 μM Fluo-3 in the absence, and presence of 55 mg/ml aldolase. (*A*) 0 Ca^{2+} spectra; (*C*) sat. Ca^{2+} spectra; (*E*) Ca^{2+} difference spectra. Right-hand side (viscosity = 2 cP): absorbance spectra of 20 μM Fluo-3 in the aldolase-free and aldolase-bound ("saturating aldolase") forms. The saturating aldolase spectra (*dashed curves*) were calculated for each of two conditions (0 Ca^{2+}, panel *B*; sat. Ca^{2+}, panel *D*) from (i) pairs of spectra of the type shown on the left-hand side, measured in the absence and presence of 55 mg/ml aldolase at the corresponding Ca^{2+} level, and (ii) the fraction of the indicator estimated to be protein-bound at 55 mg/ml aldolase. These fractions were calculated from the best-fit parameters of Scheme 1 given in the text, and were 0.735 (0 Ca^{2+} solution) and 0.426 (sat. Ca^{2+} solution). Thus, for the 0 Ca^{2+} condition (*A* and *B*), the saturating aldolase spectrum ($A_{ald}(\lambda)$) was calculated from the spectra measured in 0 and 55 mg/ml aldolase (spectra denoted $A_0(\lambda)$ and $A_{55}(\lambda)$, respectively) by the equation: $A_{ald}(\lambda) = (A_{55}(\lambda) - 0.265A_0(\lambda))/0.735$. For the sat. Ca^{2+} condition (*C* and *D*), the saturating aldolase spectgrum was calculated by the equation: $A_{ald}(\lambda) = (A_{55}(\lambda) - 0.574A_0(\lambda))/0.426$. The dashed spectra shown in *B* and *D* were obtained as the average of two runs, one at 1.6 cP (spectral pairs shown on the left-hand side) and another at 2.2 cP (spectral pairs not shown). The Ca^{2+} difference spectra in *F* are the difference between the corresponding sat. and 0 Ca^{2+} spectra in *B* and *D*.

TABLE 1 Fluo-3 Fluorescence at different values of pH

pH	F_{min}	F_{max}	F_{max}/F_{min}
A. Lot 10B-1			
6.8	66.8 ± 0.3 (n = 5)	2742.2 ± 17.3 (n = 5)	41.1 ± 0.4 (n = 5)
7.0	59.2 ± 0.7 (n = 7)	2816.8 ± 7.8 (n = 7)	47.6 ± 0.6 (n = 7)
7.5	54.8 ± 1.0 (n = 5)	2823.1 ± 10.0 (n = 5)	51.5 ± 1.0 (n = 5)
B. Lot 10D-1			
6.8	63.9 ± 0.5 (n = 3)	12,025 ± 82 (n = 3)	188.2 ± 2.4 (n = 3)
7.0	57.6 ± 1.7 (n = 3)	11,971 ± 126 (n = 3)	207.8 ± 6.1 (n = 3)
7.5	43.6 ± 2.0 (n = 3)	12,329 ± 21.9 (n = 3)	282.8 ± 13.1 (n = 3)

In vitro measurements were made from two lots of Fluo-3: Lot 10B-1 (A) and Lot 10D-1 (B). Column 1 gives the values of pH examined. Columns 2 and 3 give the Fluorescence intensity measured in 0 Ca^{2+} and sat. Ca^{2+} solutions, respectively (viscosity = 1.1 cP). These values are reported in arbitrary units that are proportional to Fluorescence intensity. Column 4 gives the ratio, F_{max}/F_{min}. For part A, the capillary diameter was 150 μm and $[D_T]$ was 0.06 mM; for part B, the capillary diameter was 200 μm and $[D_T]$ was 0.10 mM. Fluorescence intensities in parts A and B are not comparable because of differences in incident light intensity. All measurements within either part of the table were made from the same vial of Fluo-3. Different vials from the same lot revealed slightly larger variations than indicated by the table. For example, for four vials from lot 10D-1, the value of F_{max}/F_{min} varied between 175 and 225 (n = 8) at pH 7.0.

in the location of the peak absorbance and a reduction of ~8% in the amplitude of the peak. In a sat. Ca^{2+} solution (panel *C* of Fig. 2), the shift in the peak location was smaller (~2 nm), whereas the decrease in amplitude was larger (~13%). Panel *E* shows that the shape of the Ca^{2+} difference spectrum was altered markedly by 55 mg/ml aldolase. As will be discussed shortly, the Ca^{2+}-difference spectrum observed in the presence of aldolase reflects an incomplete binding reaction between Fluo-3 and aldolase at the concentrations used for these measurements (20 μM Fluo-3, 55 mg/ml aldolase).

Fluorescence. Fluorescence intensities were measured in buffer solution at aldolase concentrations between 0 and 122 mg/ml. For these measurements, the viscosity of all solutions was maintained approximately constant at 2 cP by proportional reductions in the sucrose concentration. As

shown in Fig. 3 *A*, the value of F_{MIN} (*diamonds*) increased with increasing aldolase concentration, while that of F_{MAX} (*circles*) remained approximately constant or decreased slightly. Fig. 3 *B* shows that F_{MAX}/F_{MIN} decreased from 174 in 0 mg/ml aldolase to 114 in 122 mg/ml aldolase. At aldolase concentrations of 50–90 mg/ml, i.e., in the range of the soluble protein concentration of myoplasm (10), the estimated values of F_{MAX}/F_{MIN} are 140–120.

Estimation of the aldolase:Fluo-3 dissociation constant. A binding reaction between Fluo-3 and aldolase is presumed to underlie the effects observed in panels *A*, *C*, and *E* of Fig. 2 and in panels *A* and *B* of Fig. 3. It was therefore of interest to estimate the apparent dissociation constant (K) of the aldolase:Fluo-3 reaction. In principle, the increase in F_{MIN} with increasing aldolase concentration (Fig. 3 *A*) might be used to estimate the value of K in the absence of Ca^{2+} (cf. Refs. 1 and 9). However, the increase in F_{MIN} is not large and might reflect, at least in part, the presence of contaminant Ca^{2+} in the aldolase. Thus, measurements of the indicator's Fluorescence emission anisotropy (a) were used to estimate the value of K in saturating Ca^{2+} (Fig. 3 *C*).

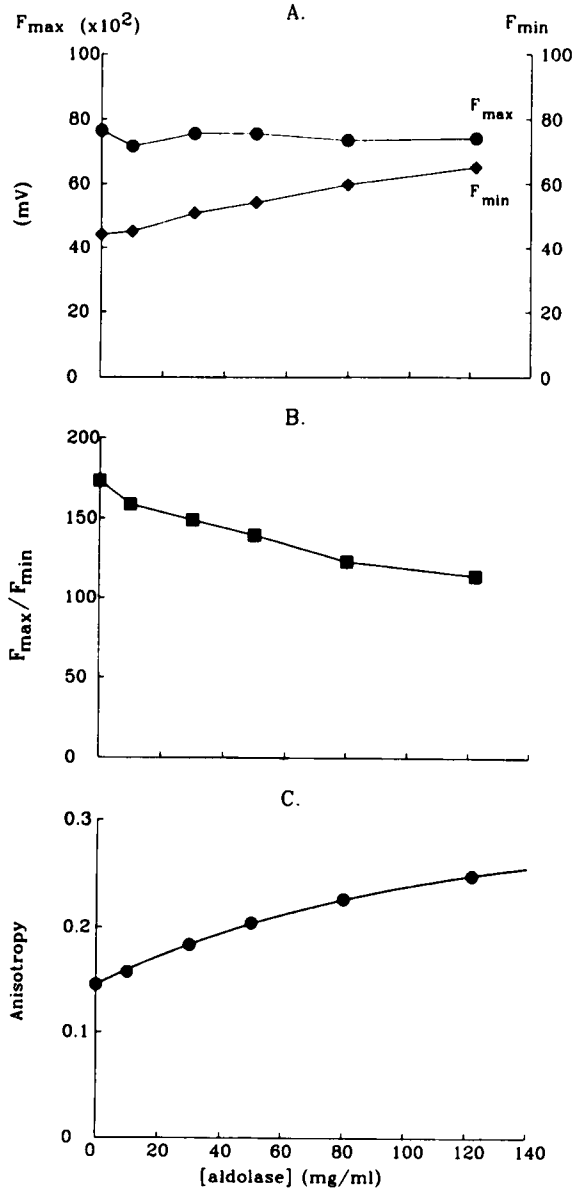

FIGURE 3 Fluo-3 Fluorescence signals (*ordinates*) measured in buffer solution containing 100 μM Fluo-3 and different concentrations of aldolase (*abscissa*). (*A*) F_{MIN} and F_{MAX} (*diamonds* and *circles*, respectively, in arbitrary units proportional to intensity). (*B*) F_{MAX}/F_{MIN}, from the data in *A*. (*C*) Fluorescence emission anisotropy (*circles*) measured in a sat. Ca^{2+} solution. In *A* and *B*, the data points have been connected by straight lines. In *C*, the curve is a least-squares fit of the data by the theory described in the text, whereby the dissociation constant (K) of aldolase for Ca^{2+}-bound Fluo-3 was estimated to be 1378 μM.

In Fig. 3 *C*, a increases progressively with increasing aldolase concentration, an effect similar to that previously observed with fura-2 (9) and fura red (1). This increase in a is presumed to reflect a decrease in the rotational mobility of the indicator when in the aldolase-bound form (cf. Ref. 12). The curve in Fig. 3 *C* is based on a previous theory (9), which assumes that each aldolase molecule can independently bind up to N indicator molecules at equivalent sites characterized by a single dissociation constant, K. For the fit in Fig. 3 *C*, it was assumed that $N = 3$ (the value that previously gave good fits in similar analyses carried out with fura-2 and fura-red), that F_{MAX} was the same whether Fluo-3 was protein-free or protein-bound (cf. Fig. 3 *A*) and that a_{ALD}, the value of a when all the indicator molecules are bound to aldolase, was 0.30. This choice of a_{ALD} is somewhat arbitrary but was based on the observations that: (i) the limiting anisotropy of Fluo-3 (estimated from a Perrin plot; see "Methods") was 0.34; and (ii) the limiting anisotropy for fura-2, 0.37, was somewhat greater than a_{ALD} for fura-2, 0.31 (9). The curve in Fig. 3 *C* was then obtained by least-squares adjustment of the value of K, the fitted value being 1378 μM.

Given this value of K and the reactant concentrations used for the absorbance measurements of Fig. 2, it follows that, for the sat. Ca^{2+} measurement (*dashed curve* in Fig. 2 *C*), 0.426 of the Fluo-3 was bound to aldolase. For the 0 Ca^{2+} measurement (*dashed curve* in Fig. 2 *A*), the fraction of Fluo-3 bound to aldolase can be estimated if the Ca^{2+} dissociation constants of aldolase-free and aldolase-bound indicator are known. A complete reaction scheme of Ca^{2+}, aldolase, and Fluo-3, for which these constants are estimated, is considered below (cf. Scheme 1).

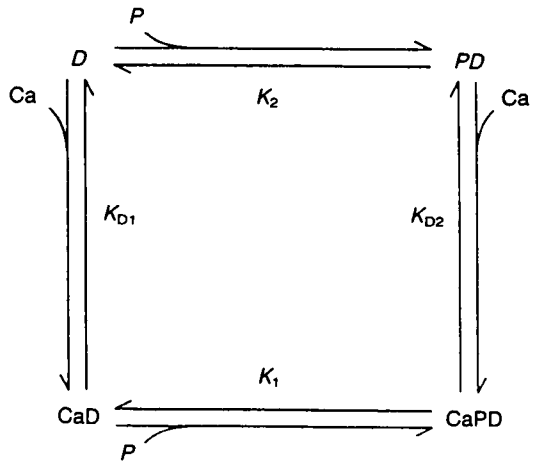

SCHEME 1

Estimation of Fluo-3's apparent dissociation constant for Ca^{2+}

The purpose of this section was to measure the apparent K_D of Fluo-3 for Ca^{2+} in the absence and presence of 55 mg/ml aldolase. In both conditions, the Fluorescence intensity data (Fig. 4 *A*: without aldolase (*open circles*); with 55 mg/ml aldolase (*filled circles*)) were well-fitted by a 1:1 binding curve (Equation 1, Methods) after K_D was adjusted to give a least-squares fit of the functional form to the data (*curves* in Fig. 4 *A*). In the absence of aldolase, K_D was 0.51 μM, comparable to the 0.40 μM value reported previously (4) for similar solution conditions (0.1 M KCl; 22°C; pH, 7.0–7.5). In the presence of aldolase, the apparent K_D was 2.1 times larger, 1.09 μM. The increase in apparent K_D observed in 55 mg/ml aldolase is somewhat less than that reported for fura-2 and fura red, where K_D increased by factors of 3.3 (9) and 4.4 (1), respectively.

Combined reaction of Ca^{2+} and aldolase with Fluo-3

Scheme 1 shows a minimal reaction scheme for the interaction of Ca^{2+}, aldolase and Fluo-3 (cf. 9). Here, the unbound forms of Ca^{2+}, aldolase, and Fluo-3 are denoted Ca, P (for protein), and D (for dye), respectively; whereas Ca^{2+}:Fluo-3 complex, aldolase:Fluo-3 complex, and Ca^{2+}:aldolase:Fluo-3 complex are denoted CaD, PD, and CaPD, respectively. The dissociation constants of the four reactions are denoted K_{D1}, K_{D2}, K_1, and K_2, as indicated.

As estimated above, K_{D1} = 0.51 μM and K_1 = 1378 μM. Since the law of mass action requires that $K_2 \times K_{D2} = K_1 \times K_{D1}$ (= 703 μM^2), the Ca^{2+}-titration data obtained in the presence of aldolase (*filled circle* data in Fig. 4 *A*, replotted in Fig. 4 *B*) can be fitted by a curve predicted from Scheme 1 with adjustment of one parameter only, either K_2 or K_{D2}. The result of this fit is shown as the dashed curve in Fig. 4 *B*, carried out under the assumptions that F_{MAX} did not change with the binding of Fluo-3 to aldolase, whereas F_{MIN} increased by a factor of 2 (cf. Fig. 3 *A*). The best-fit estimates were 366 for K_2 and 1.92 μM for K_{D2}. If the assumptions were made that neither F_{MAX} nor F_{MIN} changed with protein binding, the best-fit estimates were unchanged (fit not shown). As expected, the effective single-site K_D estimated in the presence of 55 mg/ml aldolase (cf. *dashed curve* in Fig. 4 *A*; K_D = 1.09 μM) is intermediate between the values of K_{D1} and K_{D2} assumed to apply to the complete reaction scheme (cf. *dashed curve* in Fig. 4 *B*; K_{D1} = 0.51 μM, K_{D2} = 1.92 μM).

The value estimated for the aldolase:Fluo-3 dissociation constant in the absence of Ca^{2+} (K_2 = 366 μM) is substantially larger than the analogous dissociation constant estimated in related fits with fura-2 (66 μM (9)) and fura red (69 μM (1)). The precise origin of this interesting difference in K_2 is unknown but is presumed to reflect the strength of the interaction between aldolase and the indicator's chromophore group (cf. Ref. 9, which concluded that the binding of fura-2 to aldolase likely involves the chromophore portion, rather than the Ca^{2+}-chelating portion, of the molecule).

Estimation of the absorbance spectra of aldolase-bound Fluo-3

From Scheme 1 and the values of the dissociation constants estimated above, it follows that for the conditions of the measurements in panels *A*, *C*, and *E* of Fig. 2 (55 mg/ml aldolase and 20 μM Fluo-3), 0.735 of Fluo-3 was bound to aldolase in the 0 Ca^{2+} solution and 0.426 of Fluo-3 was bound to aldolase in the sat. Ca^{2+} solution. Given these fractions, the pairs of absorbance spectra measured in Fig. 2, *A* and *C*, may be used to calculate the absorbance spectra of aldolase-bound Fluo-3 in the 0 and sat. Ca^{2+} conditions (see legend of Fig. 2). These spectra are shown as the dashed curves in panels *B* and *D* of Fig. 2; the associated Ca^{2+}

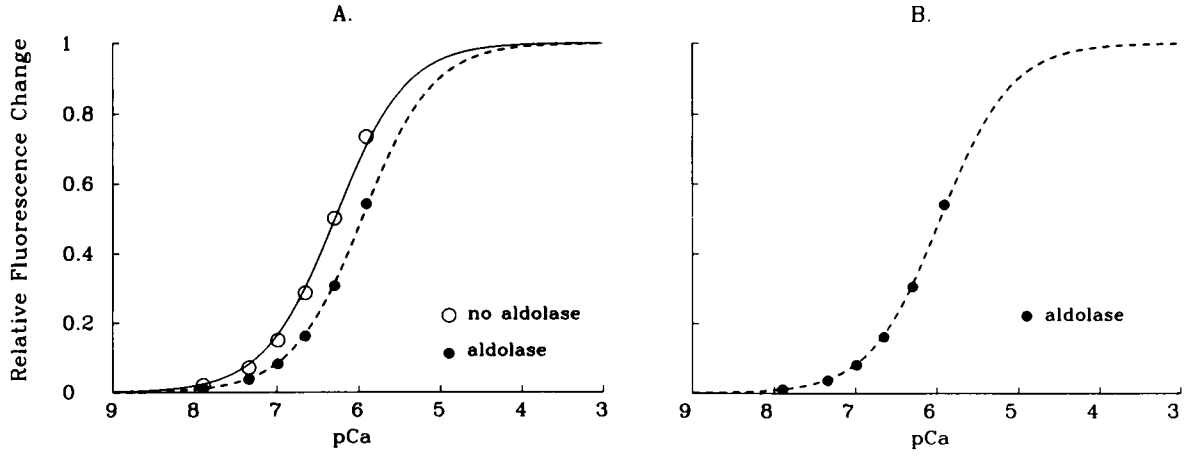

FIGURE 4 Estimation of fluo-3's apparent dissociation constant for Ca^{2+} (K_D). (*A*) The symbols show the amplitude of fluo-3's fluorescence in solutions of the indicated pCa (*abscissa*) minus that measured in a 0 Ca^{2+} solution: *open circles*, in the absence of aldolase (viscosity = 1.1 cP); *filled circles*, in the presence of 55 mg/ml aldolase (viscosity = 1.6 cP; no added sucrose). For each data set, the fluorescence changes were normalized by that measured in sat. Ca^{2+} (pCa ~2). The curves represent least-squares fits of the data by the prediction of 1:1 binding (cf. Equation 1); the best-fit K_D values were 0.51 and 1.09 μM (without and with aldolase, respectively). (*B*) Least-squares fit of the filled circle data from part *A* with the functional form predicted by Scheme 1 in the text. The best fit values of K_2 and K_{D2} were 366 and 1.92 μM, respectively, obtained under the assumption that $K_2 \times K_{D2}$ = 703 μM^2 (see text).

difference spectrum is shown as the dashed curve in panel *F*. These spectra calculated for aldolase-bound Fluo-3 are referred to below as the indicator's spectra in "saturating aldolase." It is of interest to note that the Ca^{2+} difference spectrum in saturating aldolase also has a triphasic shape; however, the isosbestic wavelengths (515 and 549 nm) are red-shifted by 11–13 nm in comparison with the isosbestic wavelengths of the 0 aldolase spectrum (504 and 536 nm; cf. Fig. 2 *F*).

Part II: In vivo measurements

Fluo-3 signals from resting fibers

Apparent diffusion coefficient. If Fluo-3 in myoplasm is not bound to muscle constituents of large molecular weight, the diffusion of the indicator along the fiber axis should be described by an apparent diffusion coefficient (D_{app}) predictable from the molecular weight of the compound. For Fluo-3 (molecular weight of 765 for the penta-valent anion), D_{app} is predicted to be $\sim 0.9 \times 10^{-6}$ cm^2 s^{-1} (16, 19, 20). If, however, Fluo-3 is bound to large and relatively immobile myoplasmic constituents such as soluble or structural proteins, D_{app} will be reduced, and the magnitude of the reduction can be used to estimate the fraction of the indicator bound to the immobile myoplasmic constituents (15, 19, 21).

The value of Fluo-3's D_{app} was estimated from the amplitude of the indicator's absorbance and/or Fluorescence signals measured at different axial distances from the site of indicator injection about 1 h after the injection (cf. Refs. 15 and 22). The absorbance measurements were made from resting fibers, whereas the Fluorescence measurements were made from either resting fibers or fibers stimulated by an action potential. The amplitude of the optical signal, which was assumed to be proportional to the concentration of indicator present at the measurement site, was least-squares fitted with the solution to the one-dimensional diffusion equation (cf. Refs. 15, 21, and 22). From the fit, two parameters were estimated: D_{app} and a second parameter M, proportional to the total quantity of fluo-3 in the fiber. The values of D_{app} so estimated in eight fibers ranged between 0.12 and 0.30×10^{-6} cm^2 s^{-1}, with the average value of D_{app} being $0.20\ (\pm\ 0.02) \times 10^{-6}$ cm^2 s^{-1}. (Note: of the eight experiments, four fibers had resting absorbance measurements only, one fiber had resting fluorescence measurements only, and three fibers had measurements of more than one type. For each experiment, a single estimate of D_{app} was obtained based on the average of all estimates available for that fiber. Of these eight fibers, three were injected with dye from lot 8E, one was injected with lot 10B-1 and four were injected with lot 10D-1. The estimates of D_{app} with lots 8E and 10B-1 represent the only in vivo measurements of this article made with a lot other than lot 10D-1.)

Since the average value of D_{app} is only $\sim$0.22 times that expected in the absence of indicator binding, $\sim$22% of the indicator molecules in myoplasm appear to be freely diffusible and $\sim$78% appear to be bound to immobile myoplasmic constituents. This percentage of bound indicator is similar to that estimated for other indicators of the tetracarboxylate family: 60–85% for fura-2 (9, 20), 80–85% for fura red (1), and $\sim$90% for azo-1 (15).

Absorbance. Fig. 5 shows an example of resting absorbance measurements from a fiber injected with fluo-3 and illustrates the procedures used to estimate the indicator-related absorbance and the indicator concentration ($[D_T]$). Similar measurements were carried out in a total of 15 fibers. Fig. 5 *A* shows the raw absorbance measurements at seven wavelengths between 480 and 630 nm. These measurements were made with two forms of linearly polarized light (*circles*, 0° polarization; *X* values, 90° polarization). At $\lambda \geq 600$ nm, the measurements reflect the intrinsic absorbance of the fiber, whereas at $\lambda < 600$ nm, the measurements reflect both the intrinsic absorbance and the indicator-related absorbance. At each $\lambda < 600$ nm, the contribution of the intrinsic absorbance was estimated from the measurements at $\lambda \geq 600$ nm (see legend of Fig. 5) and subtracted from the total absorbance to obtain the indicator-related absorbance (denoted $A_0(\lambda)$ and $A_{90}(\lambda)$ and plotted in Fig. 5 *B* as *circles* and *X*s, respectively).

If fluo-3 is not significantly bound to oriented structures in the fiber (for example, the myofilaments or the sarcoplasmic reticulum), the $A_0(\lambda)$ and $A_{90}(\lambda)$ measurements of Fig. 5 *B* should, within the error of the measurements, be equal at all λ. Conversely, if some of the indicator molecules are bound to oriented structures, the polarized absorbances may differ at one or more λ. For the fiber of Fig. 5 *B*, the A_0 data are slightly greater than the A_{90} data at four of the five wavelengths. For the 15 experiments, the mean value of the dichroic absorbance (defined as $A_0(\lambda) - A_{90}(\lambda)$) was significantly greater than zero at λ = 500, 510, and 520 nm, i.e., at the three wavelengths where the isotropic absorbance (defined as $[A_0(\lambda) + 2A_{90}(\lambda)]/3$) was relatively large. At the other two wavelengths (λ = 480 and 540 nm), the dichroic absorbance was not significantly different from zero. If averaged over all five wavelengths, the mean value of the dichroic absorbance divided by the isotropic absorbance was 0.072 ($\pm$ 0.032 SE; N = 15), a value that is also significantly different from zero. Thus, the polarized absorbance measurements suggest that a minimum of 0.072/3 = 0.024 of the fluo-3 molecules are bound to oriented structures in the fiber (cf. Ref. 23). This evidence for the binding of fluo-3 to oriented structures (see also Ref. 6) contrasts with the results of similar measurements carried out with fura red, where significant binding of fura red to oriented structures was not detected (1).

In Fig. 5 *C*, the filled circles show the isotropic absorbance (denoted $A(\lambda)$). The dashed curve in Fig. 5 *C* is fluo-3's absorbance spectrum measured in a 0 Ca^{2+}, 0 aldolase solution, scaled so as to give a least-squares fit to the fiber data. The data are not well fitted by this curve. In contrast, a good fit to the data is obtained if this same spectrum is red-shifted by 7 nm prior to the fit (*continuous curve* in Fig. 5 *C*). Panel *D* illustrates analogous fits of the same data with the 0 Ca^{2+} spectrum calculated for the saturating aldolase condition (*dashed curve* in Fig. 2 *B*). This spectral shape gives a reasonable fit to the data, both without a wavelength shift

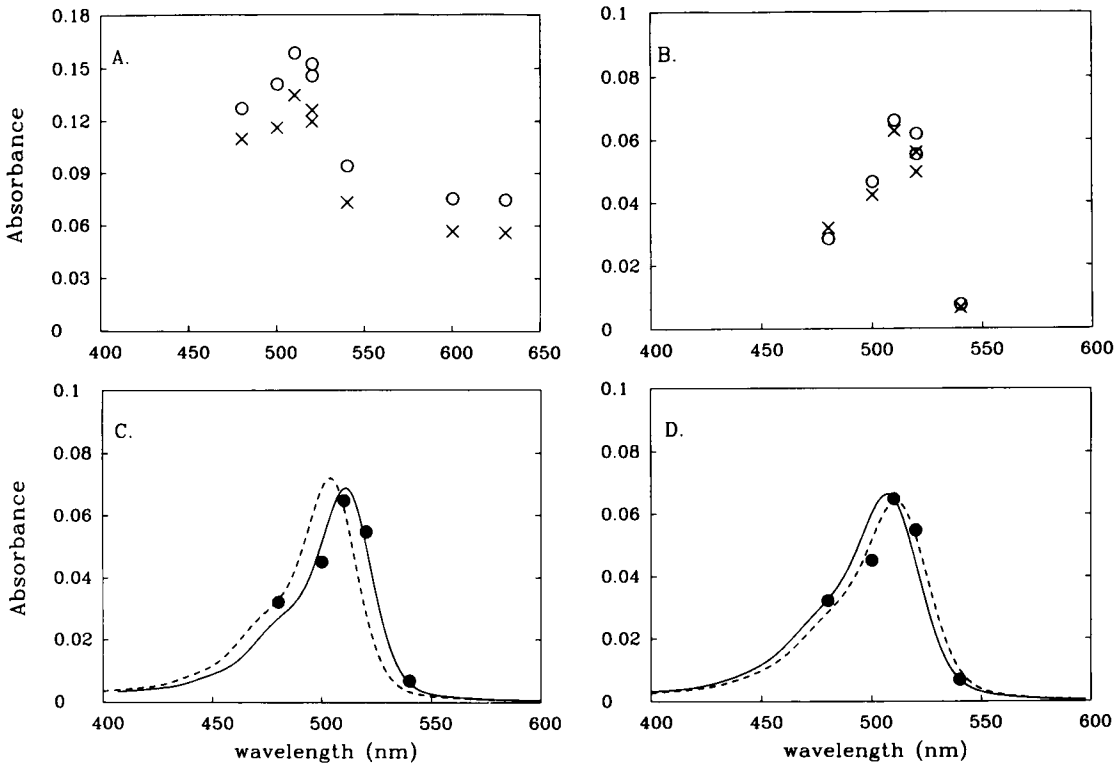

FIGURE 5 (*A*) Absorbance (intrinsic plus indicator-related) of a muscle fiber injected with ~0.12 mM fluo-3. Absorbance was measured at seven wavelengths (*abscissa*) with two forms of linearly polarized light, one oriented parallel (denoted 0°), and the other perpendicular (denoted 90°) to the fiber axis (*circles* and *X*s, respectively). (*B*) Fluo-3-related absorbance (*circles* and *X*s; absorbances denoted A_0, and A_{90}, respectively), obtained from the data in *A* by subtraction of the intrinsic absorbance; note the change in scale on the axes. At each wavelength λ the intrinsic absorbance was estimated from a scaling of $A(615)$ (= the average of the absorbances measured at 600 and 630 nm) by the factor $(\lambda/615)^Y$, where $Y = 1.1$ for the A_0 data, and $Y = 1.3$ for the A_{90} data (cf. Ref. 15). The data were also corrected, by interpolation, for a small decrease in indicator concentration during the run that resulted from the diffusion of indicator away from the measurement site. (*C* and *D*) The filled circles show the isotropic absorbance of fluo-3 (denoted $A(\lambda)$), obtained from the data points in *B* by the equation: $A(\lambda) = [A_0(\lambda) + 2 \cdot A_{90}(\lambda)]/3$. The curves in both panels represent best fits to the data with fluo-3's absorbance spectrum obtained in a 0 Ca^{2+} solution: panel *C*, 0 aldolase condition (*dashed curve*, without a wavelength shift; continuous curve with a +7-nm wavelength shift); panel *D*, saturating aldolase condition (*dashed curve*, without a wavelength shift; continuous curve with a −4-nm wavelength shift). The myoplasmic concentration of fluo-3 ($[D_T]$) estimated from the continuous curves were 122 μM in *C* and 127 μM in *D*. For calculation of $[D_T]$, the following isosbestic wavelengths and corresponding molar extinction coefficients were used: for *C*, 511 nm and 7.83×10^4 M^{-1} cm^{-1}; for *D*, 511 nm and 6.99×10^4 M^{-1} cm^{-1}. These isosbestic wavelengths represent shifts of +7 nm, and −4 nm, respectively, relative to those given in Methods for the corresponding solutions. Fiber, 062791.1; diameter, 107 μm; measurement site, 150 μm from the injection site.

(*dashed curve* in Fig. 5 *D*) and with a 4-nm blue-shift (*continuous curve* in Fig. 5 *D*). (Note: the wavelength shifts used for the fits of the *continuous curves* in Fig. 5 were obtained from the best fits of the fiber $\Delta A(\lambda)$ data with the in vitro Ca^{2+} difference spectra, as described below in connection with Fig. 7. Such wavelength shifts of indicator absorbance spectra in myoplasm are generally more reliable when evaluated from $\Delta A(\lambda)$ data than from $A(\lambda)$ data, since, as mentioned in Methods, $\Delta A(\lambda)$ data are substantially better resolved in our apparatus than are $A(\lambda)$ data.)

Estimation of $[D_T]$. The myoplasmic concentration of fluo-3 ($[D_T]$) was estimated from fits of wavelength-shifted curves of the type shown in Fig. 5 (*continuous curves*). From the fitted value of $A(\lambda)$ at the presumed isosbestic wavelength for Ca^{2+}, $[D_T]$ was calculated by Beer's law with the values of extinction coefficients given in Methods (see legend of Fig. 5). For the fiber of Fig. 5, the estimates of $[D_T]$ were 122 μM for the fit in panel *C* and 127 μM for the fit in panel *D*. For each of the other 14 fibers of Table 2, the two methods for estimation of $[D_T]$ also gave very similar estimates; on average, $[D_T]$ estimated by the method of Fig. 5 *D* was 1.050 (± 0.004; $N = 15$) times that estimated by the method of Fig. 5 *C*.

A third estimate of $[D_T]$ can be made under the assumption that the myoplasmic $A(\lambda)$ signal arises as a linear combination of the indicator's protein-free and protein-bound spectra. For example, since the D_{app} measurements suggest that ~0.8 of fluo-3 in myoplasm is bound to immobile myoplasmic constituents, $A(\lambda)$ might reasonably be approximated as 0.2 times the 0 aldolase spectrum plus 0.8 times the saturating aldolase spectrum. In general, the fiber $A(\lambda)$ data were well-fitted with such a composite spectrum, without any wavelength shift. For the fiber of Fig. 5, the value of $[D_T]$ estimated by this method was 125 μM (fit not shown), a value very similar to that obtained with the two methods illustrated in Fig. 5.

Since the estimates of $[D_T]$ obtained with the three methods were nearly identical, estimates based on one method

TABLE 2 Estimation of Δf and f_r from lot 10D-1 of fluo-3

Fiber	$[D_T]$	Δ[CaD]	Δf	$\Delta F/F$	f_r, if F_{max}/F_{min} = 100	f_r, if F_{max}/F_{min} = 200
	μM	μM				
A. 1.8 mM $CaCl_2$						
100191.2	141	80	0.57	5.4	0.096	0.101
100391.1	159	63	0.40	4.3	0.083	0.088
101791.1	164	93	0.57	5.9	0.087	0.092
101891.1	77	41	0.53	4.6	0.105	0.110
102291.1	107	63	0.59	4.4	0.124	0.129
102291.2	120	88	0.73	7.6	0.086	0.091
100792.1	40	24	0.60	6.5	0.082	0.087
Mean			0.57	5.5	0.095	0.100
$\pm$ SE (n = 7)			$\pm$0.04	$\pm$0.5	$\pm$0.006	$\pm$0.006
B. 11.8 mM $CaCl_2$						
013191.4	63	50	0.79	8.8	0.080	0.085
020691.1	129	88	0.68	8.0	0.075	0.080
020691.2	40	31	0.78	9.5	0.072	0.077
032691.4	31	13	0.42	5.7	0.064	0.069
062691.3	73	53	0.73	6.2	0.108	0.113
062791.1	122	74	0.61	6.4	0.085	0.090
082291.1	67	51	0.76	9.6	0.069	0.074
082291.2	89	64	0.72	8.8	0.072	0.077
Mean			0.69	7.9	0.078	0.083
$\pm$ SEM (n = 8)			$\pm$0.04	$\pm$0.6	$\pm$0.005	$\pm$0.005
C. Parts A and B combined						
Mean			0.63	6.8	0.086	0.091
$\pm$ SE (n = 15)			$\pm$0.03	$\pm$0.5	$\pm$0.004	$\pm$0.004

Absorbance and fluorescence measurements were made from a localized region of a single fiber injected with fluo-3 (lot 10D-1). In part A, the fibers were in normal Ringer ($[Ca^{2+}]$ = 1.8 mM); in part B, the fibers were in high Ca^{2+} Ringer ($[Ca^{2+}]$ = 11.8 mM). Column 1 gives the fiber identification number and col. 2 gives the total concentration of indicator. Columns 3–5 give the peak changes in concentration of Ca^{2+}-indicator complex, the fraction of fluo-3 complexed with Ca^{2+}, and fluo-3's fluorescence intensity resulting from action potential stimulation. f_r (columns 6 and 7) was estimated from Eq. 4 for two assumed values of $F_{max}F_{min}$: 100 (column 6) and 200 (column 7). The means and standard error of the means ($\pm$ SE) are listed below columns 4–7. Part C gives the means ($\pm$ SE) for all fibers from parts A and B.

only, that illustrated in Fig. 5 *C* (*continuous curve*), are reported for the 15 fibers (column 2 of Table 2). For all experiments, $[D_T]$ was sufficiently small, <200 μM, that $[Ca^{2+}]_r$ should not have been reduced significantly below its normal value due to the fact that indicator was injected from a solution that contained no added Ca^{2+} (cf. Ref. 1).

Fluo-3 signals in response to action potential stimulation

Absorbance changes. Fig. 6 *A* shows examples, at several incident wavelengths, of the fractional change in transmitted light intensity ($\Delta I/I$) of a fiber injected with fluo-3 and stimulated by a single action potential initiated at zero time. At each wavelength, two traces are shown, those measured with 0° (*arrowed traces*) and 90° polarized light. Fig. 6 *B* shows the 1:2 weighted average of the 0° and 90° signals at each incident wavelength after correction for the intrinsic transmission change and calibration in absorbance units (see legend of Fig. 6).

Estimation of Δ[CaD]. In Fig. 6 *B*, the wavelength dependence of ΔA is qualitatively that expected for an increase in the concentration of Ca^{2+}-fluo-3 complex (Δ[CaD]). An estimate of the amplitude of Δ[CaD] is facilitated by a comparison of the wavelength dependence of $\Delta A(\lambda)$ with that of an in vitro Ca^{2+} difference spectrum. This comparision is shown in Fig. 7. In each panel the ordinate gives the amplitude of the fiber ΔA signal (*filled circles*) at a particular λ relative to that at λ = 520 nm. At the five λ values other than 520 nm, relative signal amplitude was estimated from the scaling constant that provided a least-squares fit of the rising phase of the $\Delta A(520)$ waveform to that of the $\Delta A(\lambda)$ waveform. For the fiber of Fig. 6, and for most fibers listed in Table 2, the waveforms recorded at the different λ were very similar up until the time of their peak; after the peak, the waveforms usually differed slightly, possibly due to contamination of the traces by a movement artifact or possibly due to an unidentified component of the fluo-3 response. Thus, in general, $\Delta A(\lambda)$ amplitudes were estimated from fits of the waveforms through time to peak only.

The fiber data in the three panels of Fig. 7 are identical, whereas the curves represent best fits of the data with Ca^{2+}-difference spectra estimated for three different in vitro conditions. As in Fig. 5, a dashed curve represents the in vitro spectrum without a wavelength shift, whereas a continuous curve incorporates a shift along the wavelength axis. The shifts were +7 nm for the curve in panel *A* (0 aldolase condition) and –4 nm for the curve in panel *B* (saturating aldolase condition). These shifts represent the average of the shifts, separately estimated for each of the 15 fibers, that yielded the best least-squares fit of these spectral shapes to the fiber $\Delta A(\lambda)$ data: 7.2 ($\pm$0.1) and –3.9 ($\pm$0.1), respectively.

From (i) the values of the extinction coefficient changes given in Methods, (ii) the relative amplitude of $\Delta A(\lambda)$

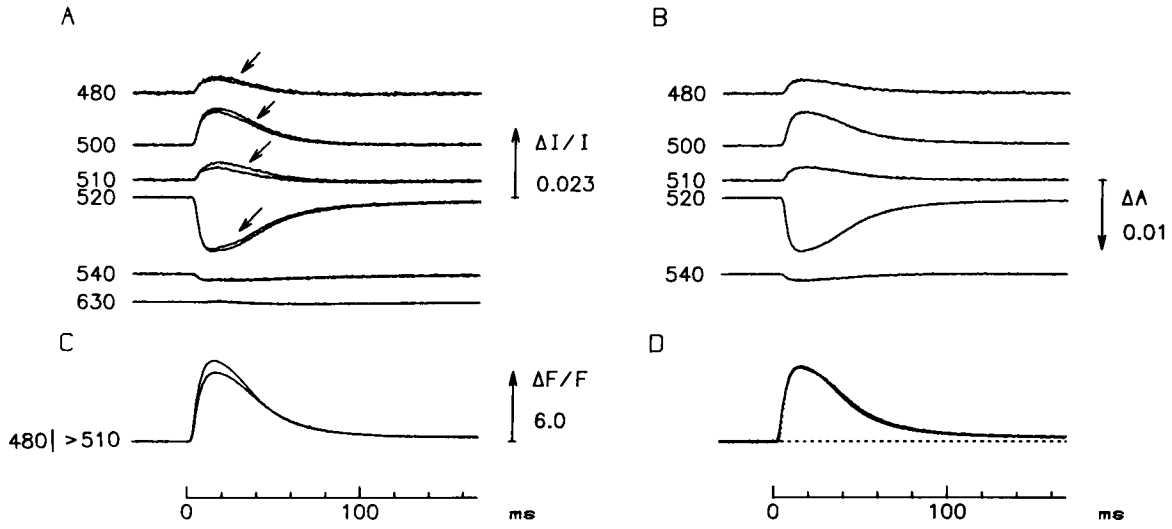

FIGURE 6 Absorbance and fluorescence changes measured in response to a single action potential. (*A*) Changes in transmitted intensity at six wavelengths (indicated in nanometers to the left). At each wavelength, the changes were measured with 0° (*arrowed traces*) and 90° polarized light. (*B*) The indicator-related isotropic absorbance changes, obtained as the 1:2 weighted average of the 0° and 90° traces from *A* after subtraction of the estimated change in fiber intrinsic absorbance. At each λ, the intrinsic change was assumed to be given by ΔA_{630} scaled by the factor $(\lambda/630)^{1.6}$. The calibration in *B* is in ΔA units $(= -(1/\ln 10)\Delta I/I)$. (*C*) The fractional change in fluo-3 fluorescence, recorded immediately before, and immediately after the records in part *A*; the larger trace was recorded first. (*D*) The average of the fluorescence traces from *C* (*continuous trace*) compared with the ΔA_{520} trace from *B* (*dotted trace*) scaled so that its peak value was the same as that of the fluorescence trace. Same experiment as Fig. 5.

calculated from the continuous curves in Fig. 7, and (iii) the absolute amplitude of $\Delta A(520)$ in Fig. 6 *B*, Δ[CaD] was estimated by Beer's law (see legend of Fig. 7). The value estimated from the fit of Fig. 7 *A* was 74 μM and from the fit of Fig. 7 *B* was 96 μM. Similar relative differences in Δ[CaD] were estimated with the two fitting procedures applied to the other fibers of Table 2. On average ($N = 15$), Δ[CaD] estimated by the method of Fig. 7 *B* (data not shown) was 1.26 (± 0.01) times that estimated by the method of Fig. 7 *A* (column 3 of Table 2). Fits based on the method of Fig. 7 *B* had substantially larger sum-of-squares deviations, on average, 6.30 (± 0.49) times larger, than those based on the method of Fig. 7 *A*. This indicates that the overall shape of the curve used in the method of Fig. 7 *A* is substantially closer to that of the muscle data than is the shape of the curve used in Fig. 7 *B*. If the extinction coefficients applicable to the curve in Fig. 7 *A* are also closer to those that apply to fluo-3 in the myoplasmic environment, then estimates of Δ[CaD] based on the method of Fig. 7 *A* will be more accurate than those based on the method of Fig. 7 *B*.

The curve in Fig. 7 *C* represents a composite Ca^{2+} difference spectrum calculated from Scheme 1 and the four absolute spectra shown in panels *B* and *D* of Fig. 2. The construction of this spectrum started from the assumption that, in the absence of Ca^{2+}, 0.2 of the fluo-3 molecules are protein-free and 0.8 are protein-bound, the approximate distribution inferred from the measurements of D_{app} (see above). The shape of the composite 0 Ca^{2+} spectrum was thus obtained as 0.2 times the 0 aldolase spectrum of Fig. 2 *B* plus 0.8 times the saturating aldolase spectrum of Fig. 2 *B*. Similarly, the composite sat. Ca^{2+} spectrum was based on a 0.48:0.52 weighting of the two sat. Ca^{2+} spectra shown in Fig. 2 *D*. The weighting for this combination was that calculated from Scheme 1 for the fraction of fluo-3 in the CaD and CaPD forms at sat. Ca^{2+} (0.48 and 0.52, respectively, if $[D_T]$ = 122 μM and [aldolase] = 84 mg/ml; this value of $[D_T]$ agrees with the estimate from Fig. 5 *A*, and the two concentrations together predict a 0.2:0.8 distribution for *D* and *PD* at 0 Ca^{2+}). The shape of the composite Ca^{2+} difference (curve in Fig. 7 *C*) was then obtained as the difference between the composite spectra calculated for sat. and 0 Ca^{2+}. Since it is clear that a scaled version of this difference spectrum would not fit the data well with any wavelength shift, no attempt was made to estimate Δ[CaD] from this fit. (Note: if a composite Ca^{2+} difference spectrum is calculated under the assumption of a partial, rather than complete, reaction of indicator with Ca^{2+}, a spectral shape indistinguishable from that shown in Fig. 7 *C* is obtained.)

The lack of agreement between the fiber data and the spectral curve in Fig. 7 *C* indicates that one or more assumptions used to construct the composite curve are inaccurate. In particular, it does not appear that there exists a single bound pool of fluo-3 in myoplasm that can be modeled with the fluo-3:aldolase reaction that was used to fit the in vitro data (Scheme 1). Thus, in myoplasm, fluo-3 may be substantially bound to muscle constituents other than aldolase (cf. the detection of indictor binding to oriented structures discussed above), or, if substantially bound to aldolase, may have properties different from those modeled by our in vitro buffer solution.

Estimation of Δf, the fractional change in Ca^{2+}-bound indicator. From the estimates of Δ[CaD] and $[D_T]$, Δf was calculated $(= \Delta[CaD]/[D_T])$. These estimates are given in column 4 of Table 2 for the fits based on the 0 aldolase spectra (cf. procedures illustrated in Figs. 5 *C* and 7 *A*). The average value of Δf observed for seven fibers in normal Ringer (part

A of Table 2) was 0.57 (± 0.04); this value is not significantly different from the 0.69 (± 0.04) value observed for eight fibers in high Ca^{2+} Ringer (part B of the Table 2).

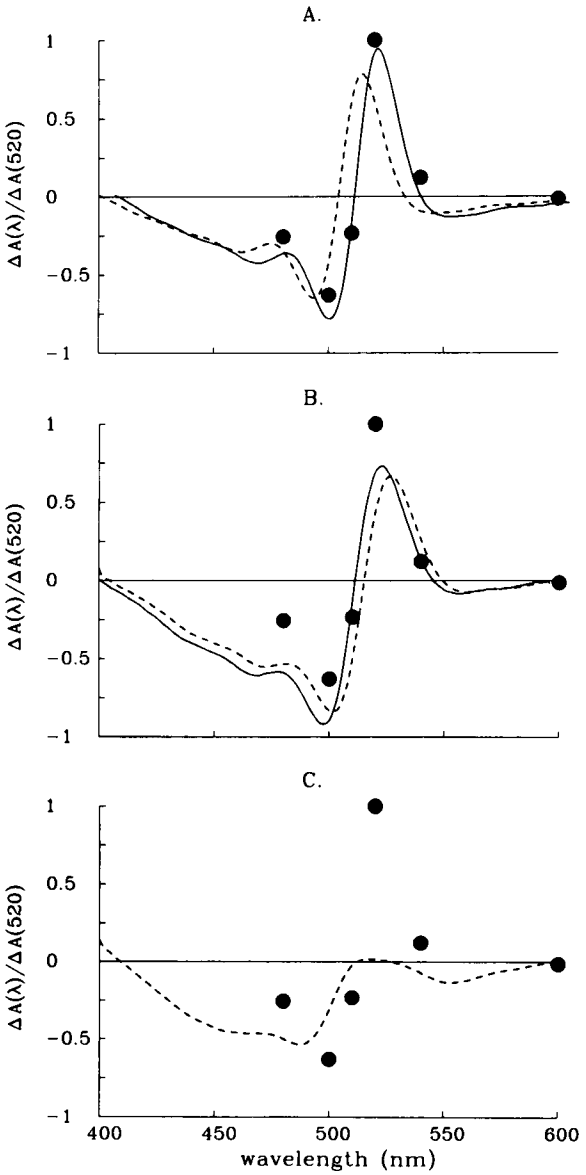

FIGURE 7 Each panel shows the normalized amplitude of the change in fluo-3's isotropic absorbance (*filled circles*) estimated from the records in Fig. 6 *B*, and compared with a Ca^{2+} difference spectrum measured in vitro (*curves*). Normalized signal amplitude was determined at each λ from the scaling constant that gave a best fit of the ΔA_{520} waveform to the $\Delta A(\lambda)$ waveform; the waveforms were fitted through time-to-peak of the ΔA_{520} waveforms (~15 ms after stimulation). All signal amplitudes were also corrected for a small drift during the run, by an interpolation based on the change in amplitude of the 520-nm signal. In *A*, the data were least-squares fitted by a 0 aldolase difference spectrum (*dashed curve*), and by this spectrum red-shifted by 7 nm (*continuous curve*). In *B*, the data were fitted by a saturating aldolase difference spectrum (*dashed curve*) and by this spectrum blue-shifted by 4 nm (*continuous curve*). The values of Δ[CaD] estimated from the fits were 74 μM (*A*) and 96 μM (*B*). The extinction coefficients used in these calculations are given in Methods (where the wavelengths of the positive and negative peaks in the difference spectrum are referenced to the unshifted curves). See text for discussion of *C*. Same experiment as Figs. 5 and 6.

Δf estimated from the saturating aldolase spectra (values not shown in Table 2; cf. Figs. 5 *D* and 7 *B*) was, on average, 1.20 (± 0.01; $N = 15$) times that estimated from the 0 aldolase spectra. As mentioned above, estimates based on the saturating aldolase spectra may be less accurate than those based on the 0 aldolase spectra because the sum-of-squares deviations of the fits were substantially larger with the former than with the latter.

Fluorescence changes. Examples of the change in fluo-3 fluorescence intensity (ΔF) measured in response to a single action potential are shown in Fig. 6 *C*. One of these records ($\Delta F/F$ at peak = 6.9) was taken immediately before, and the other ($\Delta F/F$ at peak = 5.9) immediately after, the transmission records shown in Fig. 6 *A*. The direction of ΔF is that expected for a transient increase in the concentration of Ca^{2+}-bound fluo-3. Panel *D* of Fig. 6 shows the average of the two fluorescence records from panel *C* compared with a scaled version of the $\Delta A(520)$ trace from panel *B*. The ΔA and ΔF waveforms are very similar, as expected if they both reflect Δ[CaD].

For the 15 fibers, column 5 of Table 2 gives the amplitude of $\Delta F/F$ determined at the same time as the ΔA signals used to estimate the Δ[CaD] values given in column 3 of Table 2. For fibers in normal Ringer, the average peak value of $\Delta F/F$ was 5.5 (± 0.5); for fibers in high Ca^{2+} Ringer, the average peak value was 7.9 (± 0.6). These values are statistically different; the reason for this difference is not known.

Estimation of f_r

According to Equation 4, f_r, the resting fraction of fluo-3 in the calcium-bound form, can be determined from the measurements of Δf and $\Delta F/F$ and from an assumed value of F_{MAX}/F_{MIN}. Table 2 lists f_r values estimated for the 15 fibers under two assumptions: $F_{MAX}/F_{MIN} = 100$ (column 6) and $F_{MAX}/F_{MIN} = 200$ (column 7). The latter value is that observed in a 0.1 M KCl solution at pH = 7.0 (cf. Table 1); the former value is a reasonable estimate for fluo-3 when in the aldolase-bound form (cf. Fig. 3 *B*). Given that a large fraction of fluo-3 appears to be bound to intracellular constituents of large molecular weight (see above), we think a value substantially lower than 200, but probably above 100, likely applies to fluo-3 in the myoplasmic environment. However, since both values of F_{MAX}/F_{MIN} are large, the estimates of f_r in columns 6 and 7 of Table 2 differ by only a small amount, 5–6%. For the fibers in normal Ringer, the average value of f_r is 0.095 (± 0.006) if $F_{MAX}/F_{MIN} = 100$ and 0.100 (± 0.006) if $F_{MAX}/F_{MIN} = 200$. For the fibers in high Ca^{2+} Ringer, the corresponding values are 0.078 (± 0.005) and 0.083 (± 0.005). At each value of F_{MAX}/F_{MIN}, the estimates of f_r for the two types of Ringer solution are significantly different. Again, the reason for this difference is not known. It is possible, however, that it simply represents statistical variability since (i) the difference is not large, and (ii) in analogous measurements with fura red, a difference in f_r of similar magnitude, but of opposite polarity, was found for the two types of Ringer solution (1).

Estimation of K_D in the myoplasmic environment

Because fluo-3 appears to bind heavily to myoplasmic constituents, it is likely that the effective K_D of the indicator in vivo is different from the 0.51 μM value measured in vitro in a 0.1 M KCl solution (cf. the effect of aldolase in Fig. 4 *A*). In order to estimate K_D in myoplasm, measurements of the type shown in Fig. 8 were carried out. In this experiment, the fiber was injected simultaneously with two Ca^{2+} indicators: furaptra (24) and fluo-3. Furaptra is a rapidly reacting Ca^{2+} indicator that tracks the change in myoplasmic free $[Ca^{2+}]$ in response to an action potential with little or no kinetic delay (25). In Fig. 8, the furaptra Ca^{2+} transient (*dotted traced* labeled $\Delta[Ca^{2+}]$) has a brief time course, with a time to peak of 6.0 ms and a half-width of 10.2 ms, while the fluo-3 signal (*dotted trace* labeled Δf) has a much slower time course, with a time to peak of 15.2 ms and a half-width of 47.4 ms. The slow time course of the fluo-3 signal is assumed to reflect delays imposed by the effective on- and off-rate constants of a single-site reaction of fluo-3 with Ca^{2+} (reaction rates denoted k_{+1} and k_{-1}, respectively). These rates can be estimated from the experimental traces (see legend of Fig. 8) by the method previously described for other indicators (1, 9, 26, 27). The ratio k_{-1}/k_{+1} then gives the estimate of K_D. Similar measurements were made in a total of three fibers. The average values of k_{+1}, k_{-1}, and K_D were 1.31 ($\pm$ 0.12) $\times$ 10^7 M^{-1} s^{-1}, 33.5 ($\pm$ 2.2) s^{-1}, and 2.57 ($\pm$ 0.07) μM, respectively. This in vivo estimate of K_D is 5.0 times larger than the in vitro estimate obtained in the absence of aldolase and 2.4 times larger than that obtained in the presence of aldolase (Fig. 4).

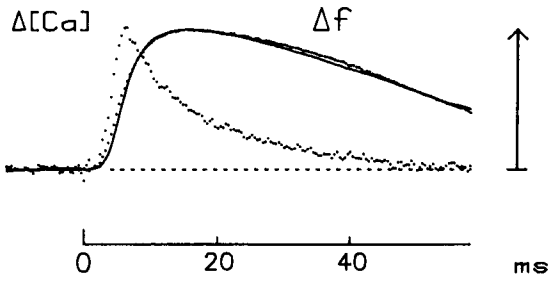

FIGURE 8 Illustration of the method used to estimate the on- and off-rate constants, and hence K_D, of the Ca^{2+}-fluo-3 reaction in myoplasm. The fiber was simultaneously injected with furaptra, and fluo-3, and stimulated at zero time to give an action potential. The trace labeled Δ[Ca] is the waveform of the free calcium transient determined from furaptra with 420-nm excitation (25); its calculation here includes correction for a small interference from fluo-3's fluorescence change at 420 nm, the amplitude of which was independently estimated in other experiments. The peak amplitude of $\Delta[Ca^{2+}]$ was 15.3 μM (after a 2-fold scaling to account for the calibration error described in Ref. 25). Two traces labeled Δf are shown. The dotted, and slightly noisier, trace is the change in the fraction of fluo-3 in the Ca^{2+}-bound form, proportional to the measured ΔF from fluo-3. The peak amplitude of Δf was assumed to be 0.656, the value estimated from the measured amplitude of $\Delta F/F$ (= 7.3) and a linear regression analysis, applied to the 15 experiments in Table 2, that related Δf and $\Delta F/F$. The continuous trace is a least-squares fit of Δf under the assumption that Δf represents a single site response driven by $\Delta[Ca^{2+}]$; the best fit values of k_{+1} and k_{-1} were 1.52 $\times$ 10^7 M^{-1} s^{-1} and 37.5 s^{-1}, respectively. The corresponding estimate of K_D ($= k_{-1}/k_{+1}$) is 2.47 μM. For the fit, f_r was assumed to be 0.082 (Equation 4), and $[Ca^{2+}]_r$ was assumed to be 0.22 μM; the latter value is consistent with an f_r of 0.082, and a K_D of 2.47 μM. Fiber 100992.1; diameter, 111 μm; measurement site, 75 μm from the injection site.

Estimation of $[Ca^{2+}]_r$

Columns 2–4 of Table 3 list estimates of $[Ca^{2+}]_r$ calculated from Equation 1 with three assumed values of K_D: 0.51, 1.09, and 2.57 μM. The value of f_r given in column 1 of the Table is that from part *C* of Table 2 for F_{MAX}/F_{MIN} = 100. (As mentioned above, we think an F_{MAX}/F_{MIN} of 100 is more likely to apply to the protein environment of myoplasm than an F_{MAX}/F_{MIN} of 200). The values of $[Ca^{2+}]_r$ in Table 3 denoted by asterisks, 103 and 242 nM, reflect the values of K_D that we think are more likely to apply to myoplasm. (As mentioned above, because fluo-3 is heavily bound to myoplasmic constituents, we think a K_D of 0.51 μM is unlikely).

ΔF in response to a train of action potentials

Previous work indicates that when a fiber is stimulated by a brief, high-frequency train of action potentials (e.g., 5–10 shocks given at 50–100 Hz), $\Delta[Ca^{2+}]$ reaches its largest value in response to the first shock, and, in response to the subsequent shocks, the average value of $\Delta[Ca^{2+}]$ reaches a quasi-steady level that is typically about 0.8 times that of the initial peak (19, 20, 25). On the other hand, Fig. 8 indicates that, with a single action potential, $\Delta[Ca^{2+}]$ is only about 0.5 of its initial peak by the time to peak of the fluo-3 signal. Thus, it is expected that, during a brief high-frequency train, fluo-3's fluorescence signal would increase slightly, perhaps ~10%, above the level reached in response to a single shock. This follows since Table 2 indicates that the peak fraction of fluo-3 in the Ca^{2+}-bound form in response to a single action potential is already large, about 0.72 (= 0.086 + 0.63; part *C* of Table 2, columns 4 and 6).

Fig. 9 shows results from an experiment designed to test this point. In response to a single shock, the peak value of $\Delta F/F$ was 6.71, whereas in response to a five-shock train given at 67 Hz, the average value of $\Delta F/F$ between the second and fifth peaks was 7.24. Thus, the average level of fluorescence achieved during the train was about 1.08 times that of the peak value resulting from a single action potential.

TABLE 3 Summary of estimates of f_r and $[Ca^{2+}]_r$ from fluo-3

	Resting $[Ca^{2+}]_r$ (nM) for the specified value of K_D (μM):		
f_r	K_D = 0.51	K_D = 1.09	K_D = 2.57
0.086	48	103*	242*

From f_r (column 1), the estimates of $[Ca^{2+}]_r$ were calculated with Eq. 1 for three assumed values of K_D. The value of f_r is that given in part C of Table 2 (column 6). The values of K_D, columns 2–4, were estimated, respectively, from in vitro measurements in the absence of aldolase (Fig. 4*A*, *open circles*), in vitro measurements in the presence of aldolase (Fig. 4*A*, *filled circles*), or from in vivo kinetic fits of the type shown in Fig. 8.

* Estimates calculated from the values of K_D that we think may apply to fluo-3 in the myoplasmic environment.

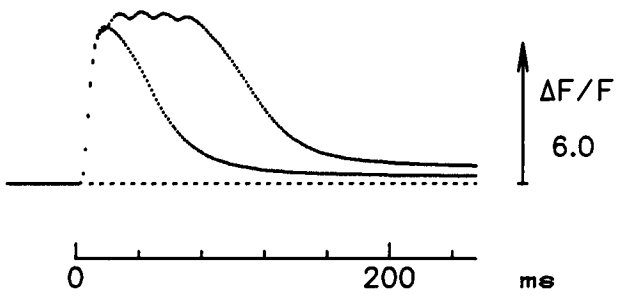

FIGURE 9 Fluo-3 fluorescence changes in response to one and five action potentials. At 0 time, the fiber was stimulated by either one shock (briefer response) or by a train of five shocks separated by 15 ms. The value of F (in arbitrary units proportional to light intensity) was 75.7 for the single-shock response and 74.7 for the five-shock response. Fiber, 020691.1; diameter, 62 μm; the measurement site was located at the injection site.

Similar results were found in a total of four fibers stimulated by a brief, high-frequency train (5–10 shocks given at 67–77 Hz). The average value of $\Delta F/F$ resulting from the second through fifth shocks was 1.12 (± 0.07) times that of the peak of $\Delta F/F$ resulting from the first shock. Overall, these results are very close to expectation and imply that, during a brief high-frequency tetanus, ~0.8 of the total fluo-3 molecules become complexed with Ca^{2+}.

Effects of elevated [K⁺] in Ringer

In experiments with aequorin, it was concluded that a Ca^{2+}-dependent luminescence signal could not be reliably detected in resting fibers in normal Ringer solution (22). If, however, the potassium concentration in Ringer ($[K^+]$) was increased from 2.5 to 12.5 mM, an increase in aequorin's luminescence was readily detected (3), which was presumed to reflect an increase in $[Ca^{2+}]_r$. The goal of the experiments described in this section was to obtain analogous information regarding the sensitivity of fluo-3's resting fluorescence signal to changes in Ringer potassium concentration.

In the experiments with fluo-3 described in the preceding sections, the fluorescence level from a fiber at rest is predicted to be 9.5 times that of F_{MIN} (if F_{MAX}/F_{MIN} is 100 and f_r is 0.086; cf. Table 3 and Equation 2). For an average sized fiber containing ~0.1 mM fluo-3, resting F is typically four to five times the amplitude of the cross-talk intensity of our apparatus (see Methods). Thus, resting F is well-resolved and a well-resolved increase in F would be expected with increases in Ringer $[K^+]$ that produce substantial increases in $[Ca^{2+}]_r$.

In Fig. 10 *A*, the abscissa shows time after injection of fluo-3 into a fiber and the ordinate shows the value of F recorded when the fiber was exposed to different $[K^+]$ levels between 2.5 and 12.5 mM. F levels recorded at 2.5 mM $[K^+]$ are shown as filled circles and at elevated $[K^+]$ as open circles. The steady decrease in the filled circle data with time is presumed to reflect a decrease in fluo-3 concentration due to the diffusion of indicator away from the measurement site. To characterize this decrease empirically, the filled circle data were fitted with a declining 2-exponential function. This fitted curve (*dashed line*) then permitted normalization of the F values recorded at elevated $[K^+]$ by the values of F that would have been measured at similar times if the fiber had been left in 2.5 mM $[K^+]$.

In the experiment of Fig. 10 *A*, increases in F were readily detected at all $[K^+]$ levels between 5 and 12.5 mM. These increases are presumed to reflect increases in $[Ca^{2+}]_r$ and indicate that fluo-3's F signal is a sensitive monitor of these

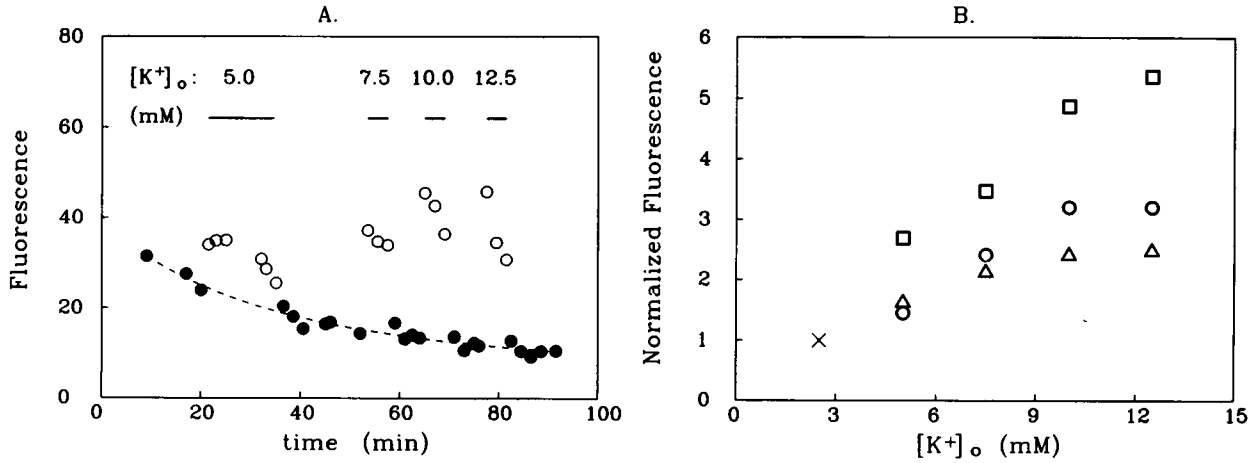

FIGURE 10 The effect of an elevation in Ringer $[K^+]$ on the fluorescence signal from fluo-3 in a nonstimulated fiber. (*A*) The ordinate plots resting fluorescence (in arbitrary units) measured at different times after the injection of fluo-3 (*abscissa*). The fiber was in high Ca^{2+} Ringer at the time of the injection and then returned to normal Ca^{2+} Ringer for the duration of the experiment. The measurements in normal Ringer (2.5 mM $[K^+]$) are shown as solid circles and the measurements in elevated $[K^+]$ Ringer are shown as open circles. The periods in elevated $[K^+]$ and the values of $[K^+]$, are indicated at the top of the panel. The dashed curve is a best fit of the filled circle data with a declining 2-exponential function ($F = F_1 \times \exp(-t/\tau_1) + F_2 \times \exp(-t/\tau_2)$). Fiber 100191.2; diameter, 63 μm; measurement site, 50 μm from the injection site. (*B*) Normalized fluorescence values (see text) calculated from the experiment of part *A* (*circles*) and from two other experiments (*triangles*, fiber 100391.2; *squares*, fiber 100391.1) plotted as a function of Ringer $[K^+]$. By definition, the normalized F value at 2.5 mM $[K^+]$ was 1.0 for all fibers (denoted X in the plot).

increases. Similar results were found in two other fibers. In one of these fibers (100391.2), F levels at $[K^+] \geq 10$ mM clearly decayed more rapidly than F levels in 2.5 mM $[K^+]$ (i.e., as seen in the fiber of Fig. 10 *A*). The reason for these decays in F is not known but is presumed to reflect a decline in the elevated $[Ca^{2+}]_r$ level produced by the elevated $[K^+]$.

For each of the fibers studied in elevated $[K^+]$ Ringer, an average "normalized F value" was calculated from all available measurements at each of the elevated $[K^+]$ levels (three to six data points/fiber/elevated $[K^+]$ level, which were measured over periods of 3–14 min and normalized to the predicted F values in 2.5 mM $[K^+]$). For the three fibers, the normalized F values (Fig. 10 *B*) varied from 1.5 to 2.7 at $[K^+] = 5$ mM, 2.1 to 3.5 at $[K^+] = 7.5$ mM, 2.4 to 4.9 at $[K^+] = 10$ mM, and 2.5 to 5.4 at $[K^+] = 12.5$ mM. Under the assumption that $F_{MAX}/F_{MIN} = 100$ and $f_r = 0.086$, the means of the normalized F levels recorded in 5, 7.5, 10, and 12.5 mM $[K^+]$ correspond to f_r levels of 0.172, 0.249, 0.326, and 0.345, respectively. The corresponding levels of $[Ca^{2+}]_r$ are, respectively, 2.2, 3.5, 5.1, and 5.6 times the value of $[Ca^{2+}]_r$ in 2.5 mM $[K^+]$ (independent of the choice of K_D).

DISCUSSION

A novel method for estimation of $[Ca^{2+}]_r$ with fluo-3

This article describes absorbance and fluorescence measurements with fluo-3, both from in vitro calibration solutions and from single muscle fibers injected with the indicator. An unexpected finding of the in vitro measurements was that F_{MAX}/F_{MIN} was ~200 (at least for the principal lot of the indicator used for the measurements of this article), a value nearly 5-fold larger than previously reported (4). The large value of F_{MAX}/F_{MIN} provides the basis for a novel calibration procedure for estimation of f_r (the fraction of fluo-3 in the Ca^{2+}-bound form in a resting fiber). The procedure has the advantage that it does not employ invasive or irreversible techniques to estimate F_{MAX} and F_{MIN} in the myoplasm, but it has the disadvantage that it is technically somewhat cumbersome. According to Equation 4 in Methods, f_r can be calculated from three quantities: (i) Δf, the change in the fraction of Ca^{2+}-bound fluo-3 in response to electrical stimulation; (ii) $\Delta F/F$, the fractional change in fluorescence in response to electrical stimulation; and (iii) a correction term equal to $(1 - F_{MAX}/F_{MIN})^{-1}$. Although the exact value of F_{MAX}/F_{MIN} in myoplasm is not known, the correction term is likely to be small since F_{MAX}/F_{MIN} exceeded 100 in the various in vitro calibrations, including those carried out in the presence of a large concentration of aldolase (122 mg/ml).

With the average concentration of fluo-3 used in the experiments, ~0.1 mM, the measurements of F and ΔF are well-resolved in our apparatus. Thus, the principal uncertainty in the estimation of f_r arises in the estimation of Δf. Δf is calculated as the ratio of two quantities, Δ[CaD] (the change in concentration of Ca^{2+}:fluo-3 complex in response to an action potential) and $[D_T]$ (the total indicator concentration). Estimation of these concentrations depends on measurements of fluo-3's absorbance, both at rest (A) and during activity (ΔA). In frog single muscle fibers, the resolution of both of these signals by our apparatus is sufficient to permit estimation of $[D_T]$ (from A) and Δ[CaD] (from ΔA). (It should be noted, however, that technical difficulties are expected in the measurement of A and ΔA in cells of smaller diameter and/or with smaller-sized Ca^{2+} transients.)

The estimation of Δf also depends on the values assumed for the indicator's molar extinction coefficients (ϵ) in the myoplasmic environment. Several findings indicate that the values of ϵ in myoplasm are not identical to the values measured in a 0.1 M KCl buffer solution: (i) fluo-3's myoplasmic spectra ($A(\lambda)$ and $\Delta A(\lambda)$) were not well fitted by the in vitro spectra unless these spectra were red-shifted by ~7 nm (if solution viscosity = 2 cP); (ii) ~0.8 of the fluo-3 molecules in myoplasm appear to be bound to myoplasmic constituents such as soluble and structural proteins; and (iii) in vitro, ϵ was altered somewhat by the addition of aldolase to the calibration solution. Interestingly, in vitro spectra measured in the presence of aldolase are characterized by a red-shift as well as a reduction in amplitude of ϵ. Somewhat surprisingly, however, the fiber $A(\lambda)$ and $\Delta A(\lambda)$ data were less well fitted with fluo-3's aldolase-bound spectra than with a red-shifted 0 aldolase spectra. The very good fits obtained with these latter spectra suggest that the estimates of Δf in Table 2 (calculated from the shifted 0 aldolase spectra) are reasonably accurate. If the Δf estimates had been calculated from the aldolase-bound spectra, they would have been larger by ~20%; this, in turn, would have increased the estimates of f_r by ~20% and of $[Ca^{2+}]_r$ by ~22%.

The remaining variable that affects the calculation of $[Ca^{2+}]_r$ is the choice of the indicator's K_D for Ca^{2+}. Two lines of evidence suggest that fluo-3's K_D in myoplasm is likely to be larger than the 0.5 μM value measured in a 0.1 M KCl solution (pH 7, 16°C). Firstly, K_D measured in the presence of 55 mg/ml aldolase was ~1.1 μM (Fig. 4). Second, a kinetic analysis of simultaneous measurements of ΔF signals from fluo-3 and furaptra in response to an action potential (cf. Fig. 9) indicated that K_D may be as large as 2.6 μM. Two possible sources of error exist in the method used to obtain the in vivo estimate of K_D: (i) the method by which the furaptra Ca^{2+} transient is calibrated, which ultimately relies on calibration of the $\Delta[Ca^{2+}]$ signal measured with purpurate indicators (purpurate diacetic acid and tetramethylmurexide (TMX); see discussion in Ref. 25), and (ii) the assumption of a spatially uniform pool of Ca^{2+} and indicator in myoplasm. Since $\Delta[Ca^{2+}]$ in response to a single action potential is likely to have substantial spatial nonuniformity (28), the estimate of K_D from the in vivo measurements could involve some inaccuracy. The estimates of $[Ca^{2+}]_r$ in Table 3 denoted with asterisks, 103 and 242 nM, reflect choices of K_D that we think are reasonable estimates for myoplasm. As discussed in Ref. 1, estimates of $[Ca^{2+}]_r$ made from highly stretched fibers (sarcomere length, ~3.8 μm) may exceed slightly (by 5–10%) estimates made from fibers at shorter sarcomere length (~2.7 μm).

The smaller of the asterisked $[Ca^{2+}]_r$ estimates in Table 3 is near the upper end of the range of values (0.02–0.12 μM) previously estimated with aequorin and Ca^{2+}-selective microelectrodes (cf. Introduction), whereas the larger of the estimates is in good agreement with the estimates obtained with fura red, 0.18–0.27 μM (1). We find it particularly interesting that $[Ca^{2+}]_r$ estimates based on the in vivo estimates of K_D (1.05 μM for fura red, 2.57 μM for fluo-3) are essentially identical with the two indicators: 0.22 μM with fura red, 0.24 μM with fluo-3 (Ref. 1 and Table 3). This finding suggests to us that $[Ca^{2+}]_r$ may indeed be close to this level since (i) the methods for estimation of f_r are very different with the two indicators, and (ii) the in vivo estimates of K_D are likely to more accurately reflect indicator properties in myoplasm than the in vitro estimates obtained in the presence of aldolase. Although we cannot absolutely exclude the possibility that $[Ca^{2+}]_r$ in our fibers is elevated due to some experimental variable, previous results with fura red suggest that elevations due to factors such as injection damage and long sarcomere length are likely to be minor (1).

Relationship of $[Ca^{2+}]$ estimates to contractile activation

The significance of a $[Ca^{2+}]_r$ level of 0.2–0.3 μM to the resting state of a skeletal muscle fiber was discussed previously (1). The experiments in this article supply new information about the level of myoplasmic $[Ca^{2+}]$ at the threshold for activation of the myofilaments (denoted $[Ca^{2+}]_t$). According to earlier work with elevated $[K^+]$ levels in Ringer (e.g. 3, 22, 29), fiber tension and/or movement becomes significant when $[K^+]$ reaches 15–20 mM. Our results with elevated Ringer $[K^+]$ (cf. Fig. 10 and last paragraph of Results) suggest that the fraction of fluo-3 in the Ca^{2+} bound form at threshold (denoted f_t) is probably ~0.4 (i.e., somewhat greater than the 0.35 average value observed at 12.5 mM $[K^+]$). Thus, according to Equation 1, $[Ca^{2+}]_t$ is predicted to be 0.67 times the K_D of fluo-3 for Ca^{2+}, or ~1.7 μM if K_D is 2.57 μM. This value of $[Ca^{2+}]_t$ is generally consistent with tension-pCa curves from skinned fibers, where, at a temperature of ~16°C, a pCa of 6.2 to 6.0 (or equivalently, a $[Ca^{2+}]$ of 0.6 to 1.0 μM) is required to activate tension to a few % of maximum, both in fibers of *Rana pipiens* (30) and *Rana temporaria* (M. A. P. Brotto and R. E. Godt, personal communication).

Our results with fluo-3, in combination with earlier findings, also supply information about the steepness of the tension-pCa relationship in intact fibers. Previous experiments (e.g. Refs. 22, 29, and 30) indicate that the level of tension achieved in response to a brief, high-frequency train of action potentials corresponds to nearly full activation of the myofilaments. As mentioned in Results, during brief, high-frequency stimulation, the fraction of fluo-3 complexed with Ca^{2+} probably rises to ~0.8, on average. Thus, nearly full activation of the myofilaments is predicted to occur when $[Ca^{2+}]$ is ~4 times the K_D of fluo-3 for Ca^{2+} (or ~10 μM if K_D is 2.57 μM). Independent of the choice of K_D, the measurements imply that the myofilaments go from threshold activation to nearly full activation as $[Ca^{2+}]$ increases by a factor of ~6 (from ~0.67 times fluo-3's K_D to ~4.0 times K_D), or, equivalently, with a change in pCa of ~0.78. This predicted steepness of the tension-pCa relationship for intact fibers is consistent with that observed for skinned fibers, where a pCa change of 0.5–0.9 is typically required to increase myofilament activation from ~5 to ~95% of maximum (e.g., Refs. 30–32).

The need for a better calibration solution to mimic the myoplasmic environment

At least 11 Ca^{2+} indicator molecules have been used to date to estimate $[Ca^{2+}]_r$ or $\Delta[Ca^{2+}]$ in frog muscle fibers (for references, see Ref. 1). With every indicator, evidence has been found that a substantial fraction of the indicator molecules is bound to intracellular constituents. Moreover, with most indicators, this binding appears to alter one or more indicator properties relevant to an accurate calibration of $[Ca^{2+}]$ (e.g., extinction coefficients, fluorescence excitation spectra, apparent K_D). Thus, it seems highly desirable to calibrate indicator properties in solutions that mimic the myoplasmic environment more closely than does a 0.1 M KCl solution. We have utilized a 0.1 M KCl solution with variable concentrations of added aldolase for this purpose (Refs. 1 and 9 and this paper). While the aldolase solutions provide useful suggestions about the way in which indicator properties might be altered by the intracellular environment, substantial uncertainty exists concerning the actual alteration.

The results of this article and of ref. 1 highlight several inadequacies of the aldolase-KCl calibration solution. For example, with fura red, the indicator's myoplasmic absorbance spectra ($A(\lambda)$ and $\Delta A(\lambda)$) were better fitted by in vitro spectra measured in the absence of aldolase than in the presence of aldolase, even though ~85% of fura red appeared to be bound to muscle constituents of large molecular weight. With fluo-3, in contrast, $A(\lambda)$ data from myoplasm were generally better fitted with in vitro spectra measured in the presence rather than the absence of aldolase (cf. *dashed curve* in Fig. 5 *D* vs. *dashed curve* in Fig. 5 *C*). On the other hand, fits of fluo-3's $\Delta A(\lambda)$ data were clearly less good if based on Ca^{2+} difference spectra measured in the presence of aldolase (cf. *curves* in panels *B* and *C* of Fig. 7) than if based on a red-shifted version of the Ca^{2+} difference spectrum measured in the absence of aldolase (*continuous curve* in Fig. 7 *A*). Thus, with both indicators, the procedures adopted to estimate $[D_T]$ and $\Delta[CaD]$ involved one or more empirical assumptions. Clearly, additional studies, both in vivo and in vitro, are required to fully characterize the behavior of indicator molecules in the myoplasmic environment.

We thank Dr. S. Hollingworth for comments on the manuscript and Dr. Graham Ellis-Davies for assistance with the high-performance liquid chromatographic analysis of fluo-3's purity.

REFERENCES

1. Kurebayshi, N., A. B. Harkins, and S. M. Baylor. 1993. Use of fura red as an intracellular calcium indicator in frog skeletal muscle fibers. *Biophys. J.* 64:1934–1960.
2. DeMarinis, R. M., H. E. Katerinopoulos, and K. A. Muirhead. 1990. New tetracarboxylate compounds as fluorescent intracellular calcium indicators. *Biochem. Meth.* 112:381.
3. Blatter, L. A., and J. R. Blinks. 1991. Simultaneous measurement of Ca^{2+} in muscle with Ca electrodes and aequorin. Diffusible cytoplasmic constituent reduces Ca^{2+}-independent luminescence of aequorin. *J. Gen. Physiol.* 98:1141–1160.
4. Minta, A., J. P. Y. Kao, and R. Y. Tsien. 1989. Fluorescent indicators for cytosolic calcium based on rhodamine and fluorescein chromophores. *J. Biol. Chem.* 264:8171–8178.
5. Grynkiewicz, G., M. Poenie, and R. Y. Tsien. 1985. A new generation of Ca^{2+} indicators with greatly improved fluorescence properties. *J. Biol. Chem.* 260:3440–3450.
6. Hollingworth, S., A. B. Harkins, and S. M. Baylor. 1990. Absorbance and fluorescence signals from fluo-3 in isolated frog skeletal muscle fibres. *J. Physiol.* 430:68P.
7. Harkins, A. B., N. Kurebayashi, S. Hollingworth, and S. M. Baylor. 1991. Absorbance and fluorescence signals from fluo-3 in intact twitch fibers from frog muscle. *Biophys. J.* 59:240*a*. (Abstr.)
8. Harkins, A. B., N. Kurebayashi, and S. M. Baylor. 1993. Resting myoplasmic free $[Ca^{2+}]$ ($[Ca^{2+}]_r$) measured with fura red and fluo-3 in intact single twitch fibers from frog skeletal muscle. *Biophys. J.* 64: 241*a*. (Abstr.)
9. Konishi, M., A. Olson, S. Hollingworth, and S. M. Baylor. 1988. Myoplasmic binding of fura-2 investigated by steady-state fluorescence and absorbance measurements. *Biophys. J.* 54:1089–1104.
10. Ottaway, J. H., and J. Mowbray. 1977. Compartmentation in control of glycolysis. *In* Current Topics in Cellular Regulation. Vol 12. B. L. Horecker and E. R. Stadtman, editors. Academic Press, Inc., New York. 107–208.
11. Baylor, S. M., and H. Oetliker. 1977. A large birefringence signal preceding contraction in single twitch fibres of the frog. *J. Physiol.* 264: 141–162.
12. Cantor, C. R., and P. R. Schimmel. 1980. Biophysical Chemistry. Part II. W. H. Freeman and Co., San Francisco, 439–444.
13. De Mello, W. C. 1973. Membrane sealing in frog skeletal muscle fibers. *Proc. Natl. Acad. Sci. USA*. 70:982–984.
14. Baylor, S. M., and H. Oetliker. 1975. Birefringence experiments on isolated skeletal muscle fibres suggest a possible signal from the sarcoplasmic reticulum. *Nature (Lond.)*. 253:97–101.
15. Baylor, S. M., S. Hollingworth, C. S. Hui, and M. E. Quinta-Ferreira. 1986. Properties of the metallochromic dyes arsenazo III, antipyrylazo III and azo 1 in frog skeletal muscle fibres at rest. *J. Physiol.* 377:89–141.
16. Kushmerick, M. J., and R. J. Podolsky. 1969. Ionic mobility in muscle cells. *Science (Wash. DC)*. 166:1297–1298.
17. Poenie, M. 1990. Alteration of intracellular fura-2 fluorescence by viscosity: a simple correction. *Cell Calcium.* 11:85–91.
18. Uto, A., H. Arai, and Y. Ogawa. 1991. Reassessment of fura-2 and the ratio method for determination of intracellular Ca^{2+} concentrations. *Cell Calcium.* 12:29–37.
19. Maylie, J., M. Irving, N. L. Sizto, and W. K. Chandler. 1987. Calcium signals recorded from cut frog twitch fibers containing antipyrylazo III. *J. Gen. Physiol.* 89:83–143.
20. Baylor, S. M., and S. Hollingworth. 1988. Fura-2 calcium transients in frog skeletal muscle fibres. *J. Physiol.* 403:151–192.
21. Crank, J. 1956. The Mathematics of Diffusion. Oxford University Press, London. 347 pp.
22. Blinks, J. R., R. Rudel, and S. R. Taylor. 1978. Calcium transients in isolated amphibian skeletal muscle fibres: detection with aequorin. *J. Physiol.* 277:291–323.
23. Baylor, S. M., M. W. Marshall, and W. K. Chandler. 1982. Dichroic components of Arsenazo III and Dichlorophosphonazo III signals in skeletal muscle fibres. *J. Physiol.* 331:179–210.
24. Raju, B., E. Murphy, L. A. Levy, R. D. Hall, and R. E. London. 1990. A fluorescent indicator for measuring cytosolic free magnesium. *Am. J. Physiol.* 256:C540-C548.
25. Konishi, M., S. Hollingworth, A. B. Harkins, and S. M. Baylor. 1991. Myoplasmic calcium transients in intact frog skeletal muscle fibers monitored with the fluorescent indicator furaptra. *J. Gen. Physiol.* 97: 271–301.
26. Baylor, S. M., S. Hollingworth, C. S. Hui, and M. E. Quinta-Ferreira. 1985. Calcium transients from intact frog skeletal muscle fibres simultaneously injected with antipyrylazo III and azo 1. *J. Physiol.* 365:70P.
27. Klein, M. G., B. J. Simon, G. Szucs, and M. F. Schneider. 1988. Simultaneous recording of calcium transients in skeletal muscle using high- and low-affinity calcium indicators. *Biophys. J.* 53:971–988.
28. Cannell, M. B., and D. G. Allen. 1984. Model of calcium movements during activation in the sarcomere of frog skeletal muscle. *Biophys. J.* 45:913–925.
29. Hodgkin, A. L., and P. Horowicz. 1960. Potassium contractures in single muscle fibres. *J. Physiol.* 153:386–403.
30. Godt, R. E., and B. D. Lindley. 1982. Influence of temperature upon contractile activation and isometric force production in mechanically skinned muscle fibers of the frog. *J. Gen. Physiol.* 80:279–297.
31. Kurebayashi, N., and Y. Ogawa. 1988. Imcrease by trifluoperazine in calcium sensitivity of myofibrils in a skinned fibre from frog skeletal muscle. *J. Physiol.* 403:407–424.
32. Brozovich, F. V., L. D. Yates, and A. M. Gordon. 1988. Muscle force and stiffness during activation and relaxation. *J. Gen. Physiol.* 91:399–420.